NASA Technical Paper 1107

Phugoid Characteristics of a YF-12 Airplane With Variable-Geometry Inlets Obtained in Flight Tests at a Mach Number of 2.9

Bruce G. Powers

DECEMBER 1977

NASA

NASA Technical Paper 1107

Phugoid Characteristics of a YF-12 Airplane With Variable-Geometry Inlets Obtained in Flight Tests at a Mach Number of 2.9

Bruce G. Powers

Dryden Flight Research Center
Edwards, California

National Aeronautics
and Space Administration

**Scientific and Technical
Information Office**

1977

PHUGOID CHARACTERISTICS OF A YF-12 AIRPLANE WITH VARIABLE-GEOMETRY INLETS OBTAINED IN FLIGHT TESTS AT A MACH NUMBER OF 2.9

Bruce G. Powers
Dryden Flight Research Center

INTRODUCTION

The YF-12 airplane is a twin-engine airplane with variable-geometry engine inlets and Mach 3 cruise capability. Reference 1 reported that difficulties were experienced in maintaining airspeed and altitude in high speed flight. The report suggested several factors that may have contributed to the piloting difficulties, including atmospheric disturbances, airplane/propulsion system interactions, and aircraft long-period dynamic characteristics. The effects of an interaction of the propulsion system, including the variable-geometry inlets, with the airplane's lateral-directional characteristics are reported in reference 2. Similarly, the effects of the propulsion system's interaction with the airplane's longitudinal characteristics needed to be investigated.

As a result, the NASA Dryden Flight Research Center conducted a series of flight tests to investigate the YF-12 airplane's short-period, phugoid, and height modes. (The height mode is an aperiodic mode due to the change in airplane characteristics with altitude. The change results primarily from the change in atmospheric density with altitude.) The tests were conducted at a Mach number of approximately 2.9 and with the propulsion system inlets in the fixed or automatic configurations. This report presents the stability and control derivatives that were obtained for the velocity and altitude degrees of freedom and the standard short-period derivatives. The effect of the inlet's configuration on the derivatives was also determined. The aircraft's modal characteristics were calculated to examine the significance of the derivatives.

SYMBOLS AND ABBREVIATIONS

Physical quantities in this report are given in the International System of Units (SI) and parenthetically in U.S. Customary Units. The measurements were taken in Customary Units.

a speed of sound, m/sec (ft/sec)

a_n normal acceleration, g

a_x longitudinal acceleration, g

$$C'_{m_{\hat{h}}} = \frac{I_y}{\bar{q}S\bar{c}} \frac{\partial M}{\partial\left(h/h_0\right)}$$

$$C'_{m_M} = \frac{I_y}{\bar{q}S\bar{c}} \frac{\partial M}{\partial\left(V/a_0\right)}$$

$$C_{m_q} = \frac{I_y}{\bar{q}S\bar{c}} \frac{\partial M}{\partial\left(\frac{q\bar{c}}{2V_0}\right)}, \text{ per rad}$$

$$C_{m_\alpha} = \frac{I_y}{\bar{q}S\bar{c}} \frac{\partial M}{\partial\alpha}, \text{ per deg}$$

$$C_{m_{\delta_{bp}}} = \frac{I_y}{\bar{q}S\bar{c}} \frac{\partial M}{\partial\delta_{bp}}, \text{ per percent}$$

$$C_{m_{\delta_e}} = \frac{I_y}{\bar{q}S\bar{c}} \frac{\partial M}{\partial\delta_e}, \text{ per deg}$$

$$C'_{X_{\hat{h}}} = \frac{m}{\bar{q}S} \frac{\partial X}{\partial\left(h/h_0\right)}$$

$$C'_{X_M} = \frac{m}{\bar{q}S} \frac{\partial X}{\partial\left(V/a_0\right)}$$

$$C_{X_\alpha} = \frac{m}{\bar{q}S} \frac{\partial X}{\partial\alpha}, \text{ per deg}$$

$$C_{X_{\delta_{bp}}} = \frac{m}{\bar{q}S} \frac{\partial X}{\partial\delta_{bp}}, \text{ per percent}$$

$$C_Z = \frac{mV_0}{\bar{q}S} Z$$

C'_{Z_h} $= \frac{mV_0}{\bar{q}S} \frac{\partial Z}{\partial\left(h/h_0\right)}$

C'_{Z_M} $= \frac{mV_0}{\bar{q}S} \frac{\partial Z}{\partial\left(V/a_0\right)}$

C_{Z_α} $= \frac{mV_0}{\bar{q}S} \frac{\partial Z}{\partial \alpha}$, per deg

$C_{Z_{\delta_{bp}}}$ $= \frac{mV_0}{\bar{q}S} \frac{\partial Z}{\partial \delta_{bp}}$, per percent

$\bar{c}$ mean aerodynamic chord, m (ft)

D_1 weighting matrix for observation vector

DPR duct pressure ratio, $\frac{\text{Static pressure}}{\text{Total pressure}}$

$\bar{d}$ average derivative value

d_i derivative value

g acceleration due to gravity, m/sec^2 (ft/sec^2)

h altitude, m (ft)

I_y moment of inertia about pitch axis, kg-m^2 (slug-ft^2)

j $= \sqrt{-1}$

M $= \frac{\text{Pitching moment}}{I_y}$, rad/sec^2

M_∞ Mach number

M_{x_i} $= \frac{\partial M}{\partial x_i}$ where $x_i = h, q, V, \alpha, \delta_{bp}, \delta_e$

m mass, kg (slugs)

N number of parameters

q	pitch rate, deg/sec or rad/sec
$\bar{q}$	dynamic pressure, N/m^2 (lb/ft^2)
S	reference wing area, m^2 (ft^2)
SAS	stability augmentation system
s	sampling rate, points/sec
T	total observation time, sec
t	time, sec
u	uncertainty level
$\bar{u}$	average uncertainty level
V	velocity, m/sec (ft/sec)
W	airplane gross weight, N (lb)
W_i	weighting function
X	$= \frac{\text{Force along } X\text{-axis}}{m}$, m/sec^2 (ft/sec^2)
X_{x_i}	$= \frac{\partial X}{\partial x_i}$ where $x_i = h, V, \alpha, \delta_{bp}, \delta_e$
y	calculated observation vector
Z	$= \frac{\text{Force along } Z\text{-axis}}{mV_0}$, rad/sec^2
Z_{x_i}	$= \frac{\partial Z}{\partial x_i}$ where $x_i = h, q, V, \alpha, \delta_{bp}, \delta_e$
z	measured observation vector
α	angle of attack, deg or rad
β	angle of sideslip, deg
Δ	incremental change
δ_{bp}	incremental bypass door movement, percent of maximum travel

δ_e	elevator position, deg
ζ	damping ratio
θ	pitch angle, deg or rad
ρ	atmospheric density, kg/m^3 ($slug/ft^3$)
τ	height mode time constant, sec
ω_d	damped natural frequency, rad/sec
ω_n	natural frequency, rad/sec

Superscript:

$[\ ]^*$	matrix transpose

Subscript:

0	average condition

A dot over a quantity denotes the time derivative of that quantity.

AIRPLANE DESCRIPTION

The YF-12 aircraft (figs. 1 and 2) is a twin-engine, delta-wing airplane with Mach 3 cruise capability. The propulsion system consists of two J58 engines with axisymmetric, variable-geometry, mixed-compression inlets. Normal-shock position in the inlet is controlled by the movement of the centerbody spike and the bypass doors located on the forward part of the nacelle. As shown in figure 3, spike position and duct pressure ratio are commanded by the inlet computer as functions of Mach number, angle of attack and sideslip, and normal acceleration. The bypass doors are operated in a closed-loop manner to maintain the commanded duct pressure ratio. For short-period maneuvers, such as elevator pulses during which Mach number is nearly constant, the bypass doors and spike move together primarily as a function of angle of attack. In phugoid maneuvers, where the airplane changes primarily in Mach number and altitude, the bypass doors and spike move primarily as a function of Mach number.

Elevons provide pitch and roll control. Elevator deflection was taken as the average symmetric deflection of the elevons, and aileron deflection was taken as the average differential deflection of the elevons. Yaw control was provided by two all-movable vertical tails. A stability augmentation system (SAS) provided some artificial stability in pitch and yaw and rate damping in pitch, roll, and yaw.

INSTRUMENTATION

The airplane parameters measured included pitch attitude, pitch angular rate, normal and axial linear acceleration at the center of gravity, and elevon and bypass door position. The instrumentation was alined with the aircraft body axis (fig. 4). Velocity, altitude, and angle of attack were derived from measurements of pressure and temperature at the nose boom. The pressure measurement used to derive angle of attack was corrected to the center of gravity location. A time lag correction of 0.4 second was obtained from reference 3 and applied to angle of attack for the flight conditions of this study. The repeatability of the parameter measurements was within the resolution of the digital recording system. The resolution of this system is indicated in the following table:

Parameter	Recording system resolution
α, deg	0.05
V, m/sec (ft/sec) . . .	1.0 (3.4)
q, deg/sec	0.04
θ, deg	0.06
h, m (ft)	3.5 (11)
a_n, g	0.010
a_x, g	0.008
δ_e, deg	0.025
δ_{bp}, percent	0.30

TEST DESCRIPTION

Three phugoid maneuvers that began at an altitude of approximately 21,900 meters (72,000 feet) and a Mach number of approximately 2.9 were analyzed. The phugoid motion was excited by opening the bypass doors to the full open position for approximately 10 seconds and then returning them to the trim position. The drag increment from the bypass door pulse provided phugoid oscillations with amplitudes of approximately ±0.02 in Mach number and ±600 meters (±2000 feet) in altitude. At first, elevator pulses were used to excite the phugoid motion; however, it was difficult to return the elevator to the trim position, and the resulting mistrim caused large altitude excursions. The bypass doors were much easier to return to the trim position, and using them to excite the phugoid motion resulted in oscillations centered about the trim condition. The pitch stability augmentation system and inlet control system configurations for the tests are summarized in the following table:

Case	Pitch SAS	Inlet control mode
A	On	Automatic
B	Off	Automatic
C	Off	Inlets fixed

Each phugoid maneuver had between two and three cycles of free oscillation. Roll attitude was controlled by the roll autopilot to preclude inadvertent inputs to the elevator through lateral stick inputs. For the automatic inlet maneuvers, the bypass doors modulated about a scheduled position. For the fixed inlet maneuvers, a bypass door position 18 percent above the nominal value was used to provide an inlet stability margin during the tests. For all maneuvers, the automatic fuel sequencing system kept the center of gravity approximately constant at $0.24\bar{c}$.

Eight elevator pulses were performed with the pitch stability augmentation system off to determine the airplane's short-period characteristics. The inlet control system configurations for these cases are shown in the following table:

Case	Inlet control mode
A1, A2	Automatic
B1, B2	Automatic
C1, C2	Inlets fixed
D, E	Inlets fixed

Cases A1 and A2 were performed immediately before phugoid case A and with the same inlet control configuration. Similarly, cases B1 and B2 correspond to phugoid case B, and cases C1 and C2 correspond to phugoid case C.

METHOD OF ANALYSIS

The stability and control derivatives were determined with a maximum likelihood estimation method which was a modification of the computer program described in reference 4. The modification consisted of adding the altitude degree of freedom so that the altitude derivatives could be determined. Two methods were used to evaluate the effects of the inlets. In the first method, the standard stability and control derivatives for the fixed inlet configuration were compared to those for the automatic inlet configuration. The differences in the derivatives were attributed to the inlet. In the second method, the inlet was considered as a separate control and control derivatives corresponding to the inlet were obtained from the automatic inlet configuration maneuvers. The average bypass door position was used as the control parameter representative of the entire inlet system.

Because of the large difference in the duration of the short-period and phugoid maneuvers, the short-period maneuvers were analyzed separately. A typical short-period maneuver took approximately 20 seconds, whereas a phugoid maneuver took about 300 seconds.

The axis system used in the analysis and the positive values of the measurements are indicated in figure 4. The equations of motion used were as follows:

$$\dot{\alpha} = Z_\alpha \alpha + Z_V V + (1 + Z_q) q - \left(\frac{g}{V_0} \sin \theta_0\right)\theta + Z_h h + Z_{\delta_e} \delta_e + Z_{\delta_{bp}} \delta_{bp} + Z_0$$

$$\dot{V} = X_\alpha \alpha + X_V V - (g \cos \theta_0)\theta + X_h h + X_{\delta_e} \delta_e + X_{\delta_{bp}} \delta_{bp} + X_0$$

$$\dot{q} = M_\alpha \alpha + M_V V + M_q q + M_h h + M_{\delta_e} \delta_e + M_{\delta_{bp}} \delta_{bp} + M_0$$

$$\dot{\theta} = q + \dot{\theta}_0$$

$$\dot{h} = -V_0 \alpha + V_0 \theta + \dot{h}_0$$

$$a_n = -\frac{V_0}{g}\left[Z_\alpha \alpha + Z_V V + Z_q q + Z_h h + Z_{\delta_e} \delta_e + Z_{\delta_{bp}} \delta_{bp}\right] + a_{n_0}$$

$$a_x = \frac{1}{g}\left[X_\alpha \alpha + X_V V + X_h h + X_{\delta_e} \delta_e + X_{\delta_{bp}} \delta_{bp}\right] + a_{x_0}$$

In addition to the bias terms (Z_0, X_0, M_0, θ_0, h_0, a_{n_0}, and a_{x_0}), the initial conditions for α, V, and q were determined. For the short-period maneuvers, the derivatives Z_α, X_α, M_α, M_q, M_{δ_e}, $Z_{\delta_{bp}}$, $X_{\delta_{bp}}$, and $M_{\delta_{bp}}$ were determined, and the altitude and velocity derivatives were kept fixed at zero. For the phugoid maneuvers, the velocity, altitude, and bypass door derivatives were determined with the short-period derivatives kept fixed at the average values.

The estimation method minimized the cost functional

$\frac{1}{T}\int_0^T \left[z(t) - y(t)\right]^* D_1 \left[z(t) - y(t)\right] dt$ where the observation vectors z and y

included α, V, q, θ, h, a_n, and a_x. The values of the weighting matrix, D_1, are shown in the following table for the short-period and phugoid maneuvers:

Observation	Short-period maneuvers	Phugoid maneuvers
	Diagonal values of the D_1 matrix	
α, rad	200,000	200,000
V, m/sec (ft/sec)	0.54 (0.105)	0.22 (0.02)
q, rad/sec	1,000,000	2,000,000
θ, rad	1,000,000	200,000
h, m (ft)	0.11 (0.01)	0.0011 (0.0001)
a_n, g	100	1000
a_x, g	1000	10,000

The results of the estimation process are presented as nondimensional derivatives. Also presented are the uncertainty levels for each data point. The uncertainty levels are proportional to the Cramer-Rao bound and provide an indication of the relative uncertainty of the derivatives. Additional information on the uncertainty levels can be found in reference 5. The velocity derivatives were nondimensionalized with respect to the nondimensional velocity V/a (that is, Mach number), and the altitude derivatives were nondimensionalized with respect to the nondimensional altitude h/h_0. All the nondimensionalizing parameters ($\bar{q}$, V_0, a_0, h_0, W, and I_y) were average values for each time history.

In nondimensionalizing the phugoid derivatives, no attempt was made to separate the coefficient changes with respect to velocity and altitude from the effects due to dynamic pressure. Thus, the nondimensional Z-force derivatives, for instance, were related to the dimensional derivatives as follows:

$$Z_V = \frac{\bar{q}S}{a_0 m V_0} C'_{Z_M}$$

$$Z_h = \frac{\bar{q}S}{h_0 m V_0} C'_{Z_{\hat{h}}}$$

instead of by the following, more complete expressions:

$$Z_V = \frac{\bar{q}S}{a_0 m V_0} \frac{\partial C_Z}{\partial M} + \frac{2\bar{q}S}{m V_0^2} C_{Z_0}$$

$$Z_h = \frac{\bar{q}S}{h_0 m V_0} \frac{\partial C_Z}{\partial(h/h_0)} + \frac{1}{\rho_0} \frac{\partial \rho}{\partial h} \frac{\bar{q}S}{mV_0} C_{Z_0}$$

The short-period maneuvers were analyzed at a sampling rate of 10 points per second. A study of the effect of sampling rate on the phugoid derivatives is summarized in appendix A. The study included sampling rates from 0.1 to 10 samples per second, and a sampling rate of 2 points per second was selected on the basis of derivative uncertainty levels and computer computation time. Since the data were available at 10 samples per second, the subsequent analyses were made with 5-point averages of the original data to obtain the 2-sample-per-second data.

RESULTS AND DISCUSSION

Short-Period Characteristics

Eight maneuvers were analyzed to determine the airplane's short-period characteristics. The derivatives were obtained from elevator pulse maneuvers with average bypass door position used as an additional control parameter to represent the inlets for the automatic inlet cases. The nondimensional coefficients are shown in figure 5 and tabulated in table 1, with the exception of the inlet derivatives, which are shown in a later section. The uncertainty level for each data point is also shown. An average value from all eight maneuvers was found for each derivative for use in determining the phugoid derivatives. The technique used to find the average, which is described in appendix B, weighted each data point on the basis of its uncertainty level. Although it was possible to identify the inlet derivatives in the short-period maneuvers, no significant variations were observed in the other short-period derivatives if the inlet model was not included.

It was not possible to identify the derivatives Z_q, X_q, Z_{δ_e}, and X_{δ_e}, and they were kept fixed at zero during the analysis. A typical comparison between a flight time history and a computed time history is shown in figure 6. The computed time history used the average values of the derivatives, the flight-measured control input, and the variable bias terms. The figure shows that the average values provide a reasonable representation of the aircraft's flight characteristics.

Phugoid Characteristics

Three phugoid maneuvers were analyzed to obtain velocity and altitude derivatives for the basic aircraft. Cases A and B included the inlet as a separate controller. The inlets were fixed for the case C maneuver, so the basic airplane derivatives were obtained without having to estimate the inlet derivatives. As shown in figure 7, the fit of the computed and measured time histories is reasonably good. The velocity and altitude derivatives and the weighted averages based on the uncertainty levels are given in figure 8 and table 2(a) for the three cases. There is a considerable amount of scatter in the data, but, in general, cases A and B agree

with case C, validating the use of bypass door deflection as representative of the total inlet system.

Maneuvers A and B were also analyzed to determine the effective velocity and altitude derivatives for the combined airplane/inlet system. The computed time histories showed essentially the same fit as shown in figure 7 for the basic airplane. The resulting derivatives are summarized in figure 8 and table 2(b) and are denoted as cases $\bar{A}$ and $\bar{B}$. The differences between the derivatives for the basic airplane and the airplane/inlet system are due to the effects of the inlets. Figure 8 shows that the effects of the inlets on the Z-axis derivatives (C'_{Z_M} and $C'_{Z_{\hat{h}}}$) as well as on the pitching moment derivatives (C'_{m_M} and $C'_{m_{\hat{h}}}$) are small. As would be expected, the primary effect of the inlets is along the X-axis (which is approximately the negative thrust axis). The average value of C'_{X_M} for the basic airplane (fig. 8) is negative, indicating a stabilizing tendency with respect to speed changes. For the airplane/inlet system cases ($\bar{A}$ and $\bar{B}$, fig. 8), C'_{X_M} is positive, which would indicate a tendency for speed to diverge.

The uncertainty levels indicate that, in general, cases C, $\bar{A}$, and $\bar{B}$, in which the inlet derivatives were not identified, produced better estimates of the derivatives. Cases A and B were poorly conditioned for purposes of inlet derivative determination, since the bypass doors moved approximately with velocity, causing a nearly linear dependence between the velocity and bypass door derivatives. Some independent motion did occur because of small atmospheric disturbances, and this allowed the estimates to be made; but the uncertainty levels are greater than in cases C, $\bar{A}$, and $\bar{B}$.

In addition to the uncertainty in the phugoid derivatives that resulted from the conditioning of the phugoid maneuvers, some uncertainty in the phugoid derivatives resulted from the fact that short-period derivatives were kept fixed during the analysis of the phugoid maneuvers. The effect of each short-period derivative was evaluated by rematching one maneuver (case $\bar{A}$) with the short-period derivative increased by the value of its average uncertainty level (shown in table 1). The resulting uncertainty levels are compared with those due to the original phugoid time history match for case $\bar{A}$ in table 3. The primary short-period contribution to the uncertainty in C'_{Z_M} and $C'_{Z_{\hat{h}}}$ was from C_{Z_α}. For C'_{X_M} and $C'_{X_{\hat{h}}}$ the primary contribution was from C_{X_α} and for C'_{m_M} and $C'_{m_{\hat{h}}}$ it was from C_{m_q}. The table shows that the total short-period contribution to the uncertainty of the phugoid derivatives is small compared with the uncertainty resulting from the match of the phugoid time history, except for the effect of C_{X_α} on C'_{X_M} and $C'_{X_{\hat{h}}}$, where the two contributions are about equal. It was assumed that the uncertainties due to the short-period derivatives in the other cases were the same as those shown in table 3 for case $\bar{A}$, and when applied to the other cases these uncertainties resulted in the average velocity and altitude derivatives and the average uncertainty levels summarized in figure 9.

Inlet Derivatives

Inlet derivatives were obtained from the short-period as well as from the phugoid maneuvers, and the results are summarized in figure 10 and table 4. The weighted average shown in both the figure and the table is a weighted mean of all the points based on the uncertainty levels shown. As a result of the weighting, the average values of $C_{Z_{\delta_{bp}}}$ and $C_{X_{\delta_{bp}}}$ were primarily determined from the phugoid maneuvers, and the average value of $C_{m_{\delta_{bp}}}$ was primarily determined from the short-period maneuvers.

During the phugoid maneuvers, the inlet varied primarily with velocity. As a means of verifying the consistency of these results with the effects attributed to the inlets in the derivatives shown in figure 8, effective velocity derivatives were calculated from the inlet derivatives. A least-squares fit of the bypass door position as a function of Mach number yielded a value of $\Delta\delta_{bp}/\Delta M_\infty$ equal to -41 percent per Mach number. Effective velocity derivatives were calculated using this value. The derivatives are compared with the increments from figure 9 in the following table:

	Difference between basic airplane derivative and airplane/inlet derivative (fig. 9)	Effective velocity derivatives calculated from inlet derivative (fig. 10) and $\Delta\delta_{bp}/\Delta M_\infty$ = -41 percent per M
$\Delta C'_{Z_M}$	-0.00259	-0.0160
$\Delta C'_{X_M}$	0.0526	0.0462
$\Delta C'_{m_M}$	0.00126	0.00173

Agreement is good for $\Delta C'_{X_M}$, which is the derivative most affected by the bypass doors. The values of $\Delta C'_{m_M}$ are in reasonably good agreement. The agreement of $\Delta C'_{Z_M}$ is relatively poor, but the magnitudes are low compared with C'_{Z_M}, and the differences are not significant.

Aircraft Stability Characteristics

Eigenvalues were calculated with the derivatives of each case and with the average sets of derivatives. All the derivatives were dimensionalized to the same flight condition (M = 2.9, h = 21,900 m (72,000 ft)). One set of short-period derivatives, which produced short-period roots of $-0.17 \pm 1.16j$, was used. The

phugoid and height mode roots are shown in figure 11. Agreement is reasonably good between the roots for the individual cases and the roots from the average derivatives, with the exception of case B, the derivatives for which had large uncertainty levels (fig. 8). For the average basic airplane data, the phugoid is neutrally damped, with a period of 151 seconds. The height mode is stable, with a time to half amplitude of 99 seconds. For the average airplane/inlet system data, the phugoid is slightly divergent, with a time to double amplitude of 490 seconds and a period of 137 seconds. The height mode is divergent, with a time to double amplitude of 114 seconds.

The airplane is normally flown with a longitudinal stability augmentation system in operation. The characteristics of the phugoid and height mode roots for a linear representation of the augmentation system are shown in figure 12. Also presented are the specifications for the phugoid mode from reference 6. It is apparent that the augmentation system has little effect on the height mode but improves phugoid damping from level 3 to level 1. However, the low magnitude of the pitch rate in the phugoid maneuver with the augmentation system engaged (fig. 7), combined with the deadbands within the control system, produced essentially no feedback of pitch rate or attitude to the elevator. As a result, the augmented phugoid damping is a function of the magnitude of the oscillation. The height mode, not being a function of the stability augmentation system, is convergent for the basic airplane and divergent for the airplane/inlet system. Limited pilot evaluations of the augmented airplane with the automatic inlets (ref. 1) resulted in satisfactory (level 1) pilot ratings for the altitude hold task under stable atmospheric conditions but unsatisfactory (level 2) pilot ratings when atmospheric disturbances were present.

The effects of the velocity and altitude derivatives on the phugoid and height mode roots are shown in figure 13. The derivatives were varied about the values for the average airplane/inlet system. Also shown are the values for the average basic airplane. The figure gives an indication of the significance of the differences between the derivatives for the fixed and automatic inlets. The Z-axis derivatives (fig. 13(a)) show little effect of the inlets on the phugoid and height modes. The X-axis derivatives (fig. 13(b)) show large differences between the basic airplane and the airplane/inlet system derivatives, but X_h has little effect on either the phugoid or the height mode. The derivative X_V (a positive value indicating an increase in net propulsive force with speed) is shown to be a primary derivative for the height mode root. The pitching-moment derivatives are shown in figure 13(c). The differences in M_V due to the inlet configuration are large but have little effect on the roots. The differences in M_h have a primary effect on the phugoid frequency. Thus, when the basic airplane and the airplane/inlet system derivatives in figure 9 are compared, only the differences in C'_{X_M} and $C'_{m_{\dot{h}}}$ appear to be significant.

CONCLUDING REMARKS

The longitudinal stability and control derivatives of the YF-12 airplane were determined from flight tests at a Mach number of approximately 2.9 by using a maximum likelihood parameter estimation technique. Short-period pulses and phugoid maneuvers were analyzed to obtain the velocity and altitude derivatives as well as the short-period derivatives. Engine inlet bypass door position was successfully used to represent the total inlet system, and the effect of the inlets on the velocity and altitude derivatives was determined.

The phugoid mode of the basic airplane had neutral damping, and the height mode was stable. With the addition of inlets in the automatic configuration, the phugoid mode was slightly divergent and the height mode was divergent with a time to double amplitude of approximately 114 seconds. The results of the derivative estimation indicated that the change in the height mode characteristics was primarily the result of the change in the longitudinal force derivative with respect to velocity. The net propulsive force of the basic airplane decreased with increasing velocity, whereas the net propulsive force of the airplane/inlet system increased with increasing velocity.

Dryden Flight Research Center
National Aeronautics and Space Administration
Edwards, Calif., January 31, 1977

APPENDIX A.—REQUIREMENTS FOR TIME HISTORY

SAMPLING RATE AND LENGTH

In the determination of stability and control derivatives, there is a tradeoff between the sampling rate (or computation time) and the accuracy of the results. The tradeoff between computation time and accuracy was evaluated for the phugoid maneuver denoted case $\bar{A}$. Data acquired at a sampling rate of 10 points per second were available. Sampling rates down to 0.1 point per second were obtained by thinning the original time history. The identification algorithm was iterated until the cost functional did not change more than 0.1 percent.

The velocity and altitude derivatives and their uncertainty levels are shown in figure 14 as a function of sampling rate. Agreement between the 10-point-per-second data and the lower sampling rate data is good for sampling rates down to 1.25 points per second. Below this rate, agreement becomes poor, and at a sampling rate of 0.1 point per second the estimation method does not converge on a solution. The uncertainty level increases as sampling rate decreases; however, this may be due to the noise characteristics of the data rather than a true indication of accuracy.

For data acquired at sampling rates of 1.25 points per second and above, convergence was obtained in six iterations. At sampling rates of 0.625 and 0.25 point per second, seven iterations were required for convergence. A sampling rate of 2 points per second was chosen as a reasonable compromise between computation time and accuracy. Before the final analysis, the 10-point-per-second data were presmoothed using a simple 5-point average to obtain the 2-point-per-second data.

Another factor that affects computation time and the accuracy of the results is the length of the time history (or observation time) from which the derivatives are estimated. The phugoid maneuver of case $\bar{A}$ (with 2-point-per-second data) was used to evaluate the effects of observation time on the velocity and altitude derivatives, and the results are shown in figure 15. Since there were no control inputs and the oscillations were nearly uniform, all the time histories had the same starting point. The derivatives shown for observation time T correspond to the altitude time history shown in the figure from 0 to T. Although estimates of the derivatives were obtained for as little as one-half cycle of the phugoid oscillation (T = 60 seconds), approximately two cycles of oscillation appear to be necessary before reasonable estimates of all the derivatives can be obtained.

APPENDIX B.—USE OF UNCERTAINTY LEVELS IN THE CALCULATION OF AVERAGE DERIVATIVE VALUES

When several estimates of a derivative are available, it is desirable to use information about the relative accuracy of the estimates to obtain the best overall estimate of the derivative. The parameter estimation method in reference 4 provides an indication known as uncertainty level of the accuracy with which the derivatives have been identified. Uncertainty level is analogous to standard deviation, and further discussion of uncertainty level can be found in reference 5. For this study, an average derivative value $\bar{d}$ was determined by using a weighted average as follows:

$$\bar{d} = \frac{\sum_{i=1}^{N} W_i d_i}{\sum_{i=1}^{N} W_i}$$

where

d_i ith estimate of the derivative

W_i weighting for the ith estimate

N number of estimates

The expression for the weighting was based on uncertainty level and was given by

$$W_i = \left(\text{Uncertainty level of } d_i\right)^{-2}$$

An average uncertainty level $\bar{u}$ was determined from the weighted average

$$\bar{u}^2 = \frac{\sum_{i=1}^{N} W_i u_i^2}{\sum_{i=1}^{N} W_i}$$

where u_i is the uncertainty of derivative d_i. For the weightings used in this study,

this expression reduced to

$$\bar{u}^2 = \frac{N}{\sum_{i=1}^{N} (u_i)^{-2}}$$

REFERENCES

1. Berry, Donald T.; and Gilyard, Glenn B.: Airframe/Propulsion System Interactions—An Important Factor in Supersonic Aircraft Flight Control. AIAA Paper No. 73-831, Aug. 1973.

2. Gilyard, Glenn B.; Berry, Donald T.; and Belte, Daumants: Analysis of a Lateral-Directional Airframe/Propulsion System Interaction of a Mach 3 Cruise Aircraft. AIAA Paper No. 72-961, Sept. 1972.

3. Gilyard, Glenn B.; and Belte, Daumants: Flight-Determined Lag of Angle-of-Attack and Angle-of-Sideslip Sensors in the YF-12A Airplane From Analysis of Dynamic Maneuvers. NASA TN D-7819, 1974.

4. Maine, Richard E.; and Iliff, Kenneth W.: A FORTRAN Program for Determining Aircraft Stability and Control Derivatives From Flight Data. NASA TN D-7831, 1975.

5. Iliff, Kenneth W.; and Maine, Richard E.: Practical Aspects of Using a Maximum Likelihood Estimation Method To Extract Stability and Control Derivatives From Flight Data. NASA TN D-8209, 1976.

6. Flying Qualities of Piloted Airplanes. Military Specification MIL-F-8785B (ASG), Aug. 7, 1969.

TABLE 1.—SHORT-PERIOD DERIVATIVES

Case	Value of —	C_{Z_α}, per deg	C_{X_α}, per deg	C_{m_α}, per deg	C_{m_q}, per rad	$C_{m_{\delta_e}}$, per deg
A1	Short-period derivative	-0.028960	0.0008532	-0.0009680	-1.4510	-0.0013100
	Uncertainty level	±0.004770	±0.0021500	±0.0000109	±0.2511	±0.0000658
A2	Short-period derivative	-0.031510	0.0012890	-0.0009712	-0.9344	-0.0011500
	Uncertainty level	±0.002868	±0.0018405	±0.0000133	±0.1555	±0.0000378
B1	Short-period derivative	-0.026610	0.0015230	-0.0008586	-0.9145	-0.0008808
	Uncertainty level	±0.004756	±0.0019235	±0.0000093	±0.1737	±0.0000392
B2	Short-period derivative	-0.037660	0.0018830	-0.0008917	-0.6898	-0.0009513
	Uncertainty level	±0.011280	±0.0044365	±0.0000151	±0.3874	±0.0000718
C1	Short-period derivative	-0.026640	0.0004785	-0.0008647	-1.4520	-0.0010350
	Uncertainty level	±0.002439	±0.0019815	±0.0000171	±0.2494	±0.0000485
C2	Short-period derivative	-0.031470	-0.0000476	-0.0008802	-1.0530	-0.0009537
	Uncertainty level	±0.003916	±0.0028345	±0.0000207	±0.2579	±0.0000484
D	Short-period derivative	-0.043340	0.0013520	-0.0009257	-0.9019	-0.0011900
	Uncertainty level	±0.004632	±0.0020700	±0.0000123	±0.2174	±0.0000525
E	Short-period derivative	-0.022660	0.0008864	-0.0009715	-1.3600	-0.0010180
	Uncertainty level	±0.004797	±0.0020670	±0.0000116	±0.1951	±0.0000422
Weighted average	Short-period derivative	-0.029782	0.0010191	-0.0009200	-1.0853	-0.0010462
	Uncertainty level	±0.003845	±0.0021827	±0.0000127	±0.2134	±0.0000474

TABLE 2.—PHUGOID DERIVATIVES

(a) Basic airplane

Case	Value of —	C'_{Z_M}	$C'_{Z_{\hat{h}}}$	C'_{X_M}	$C'_{X_{\hat{h}}}$	C'_{m_M}	$C'_{m_{\hat{h}}}$
A	Phugoid derivative	-0.0590280	0.3209103	-0.0341026	0.0358694	-0.0002269	-0.0069156
	Uncertainty level	±0.0202356	±0.0432446	±0.0069617	±0.0122550	±0.0006039	±0.0013324
B	Phugoid derivative	-0.0051690	0.3621604	0.0162794	-0.0529985	0.0042093	-0.0025460
	Uncertainty level	±0.0352015	±0.0460856	±0.0141296	±0.0143139	±0.0014389	±0.0018926
C	Phugoid derivative	-0.0682926	0.2718828	-0.0276689	-0.0072000	0.0021633	-0.0008271
	Uncertainty level	±0.0359928	±0.0331589	±0.0028062	±0.0041600	±0.0010258	±0.0009657
Weighted average	Phugoid derivative	-0.0499972	0.3077680	-0.0270963	-0.0062877	0.0008304	-0.0028689
	Uncertainty level	±0.0273144	±0.0395794	±0.0044335	±0.0065784	±0.0008477	±0.0012517

(b) Airplane/inlet system

Case	Value of —	C'_{Z_M}	$C'_{Z_{\hat{h}}}$	C'_{X_M}	$C'_{X_{\hat{h}}}$	C'_{m_M}	$C'_{m_{\hat{h}}}$
$\bar{A}$	Phugoid derivative	-0.0498299	0.3185730	0.0177792	-0.0716930	-0.0008564	-0.0060487
	Uncertainty level	±0.0106757	±0.0375977	±0.0017023	±0.0088026	±0.0003428	±0.0011962
$\bar{B}$	Phugoid derivative	-0.0731338	0.4088526	0.0417087	-0.0406737	0.0048611	-0.0037563
	Uncertainty level	±0.0301993	±0.0504131	±0.0024658	±0.0066243	±0.0012091	±0.0020923
Weighted average	Phugoid derivative	-0.0524187	0.3508400	0.0255026	-0.0518891	-0.0004309	-0.0054840
	Uncertainty level	±0.0142344	±0.0426229	±0.0019811	±0.0074854	±0.0004664	±0.0014686

TABLE 3.—EFFECT OF SHORT-PERIOD DERIVATIVE UNCERTAINTIES ON PHUGOID DERIVATIVES

Short-period derivative	Uncertainty in short-period derivative, percent	Phugoid derivative					
		C'_{Z_M}	C'_{X_M}	C'_{m_M}	$C'_{Z_{\hat{h}}}$	$C'_{X_{\hat{h}}}$	$C'_{m_{\hat{h}}}$
		Uncertainty in phugoid derivative due to short-period derivative uncertainty, percent					
C_{Z_α}	12.9	4.42	2.76	0.36	7.00	2.69	0.17
C_{X_α}	214.1	0.15	8.02	0.33	0.13	16.92	0.15
C_{m_α}	1.4	0.08	0.31	1.00	0	0.29	1.22
C_{m_q}	19.7	1.36	0.14	2.81	0.66	0.44	2.23
$C_{m_{\delta_e}}$	4.5	0.17	0.81	1.92	0.03	0.64	0.03
Total uncertainty due to short-period derivatives, $\left(\sum (\text{Uncertainty})^2\right)^{1/2}$		4.63	8.53	3.58	7.03	17.16	2.55
Uncertainty due to phugoid time history match for case $\bar{A}$		21.42	9.57	40.03	11.80	12.28	19.78
Total uncertainty for case $\bar{A}$		21.91	12.82	40.19	13.74	21.10	19.94

TABLE 4.—INLET DERIVATIVES

Case	Value of —	Inlet derivatives and uncertainty levels		
		$C_{Z_{\delta_{bp}}}$, per percent	$C_{X_{\delta_{bp}}}$, per percent	$C_{m_{\delta_{bp}}}$, per percent
A	Derivative	-0.0000457	-0.0021895	0.0000321
	Uncertainty level	±0.0005731	±0.0002774	±0.0000215
B	Derivative	0.0012055	-0.0006501	0.0000019
	Uncertainty level	±0.0005095	±0.0002241	±0.0000196
A1	Derivative	0.0003262	-0.0004757	0.0000998
	Uncertainty level	±0.0021275	±0.0012145	±0.0000168
A2	Derivative	0.0003846	-0.0005902	0.0000467
	Uncertainty level	±0.0013875	±0.0011160	±0.0000084
B1	Derivative	-0.0003080	-0.0003555	0.0000387
	Uncertainty level	±0.0006220	±0.0004877	±0.0000055
B2	Derivative	0.0002862	-0.0001223	0.0000203
	Uncertainty level	±0.0038900	±0.0016910	±0.0000302
Weighted average	Derivative	0.0003887	-0.0011230	0.0000422
	Uncertainty level	±0.0007637	±0.0003925	±0.0000102

E-24984

Figure 1. YF-12 airplane.

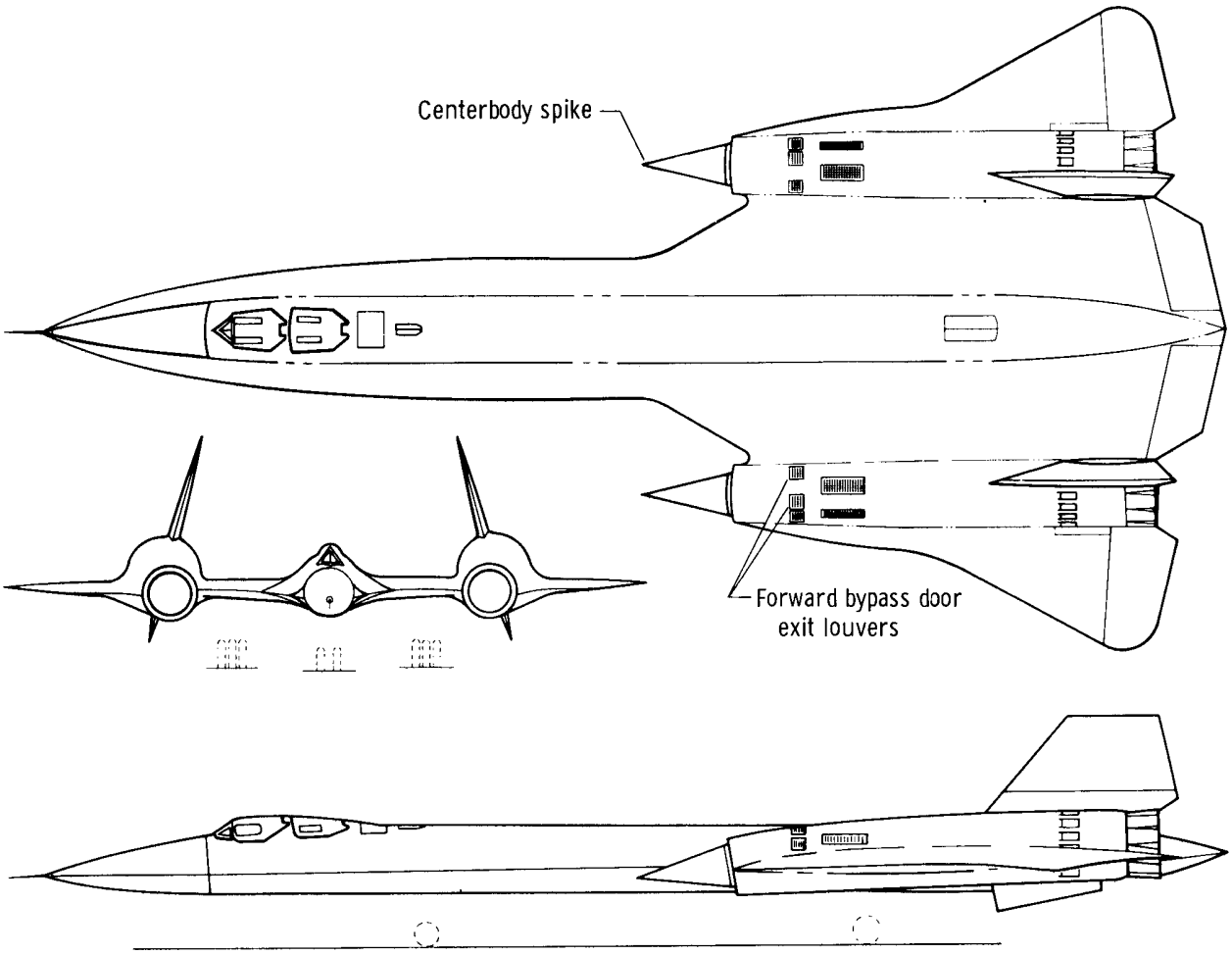

Figure 2. Three-view drawing of test airplane.

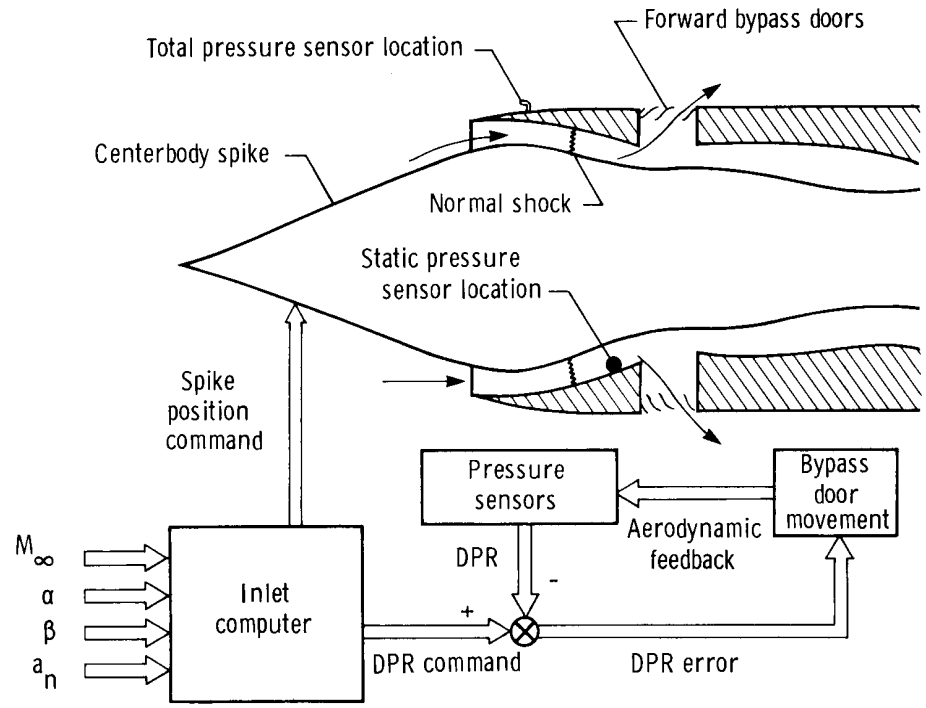

Figure 3. Schematic of inlet control system.

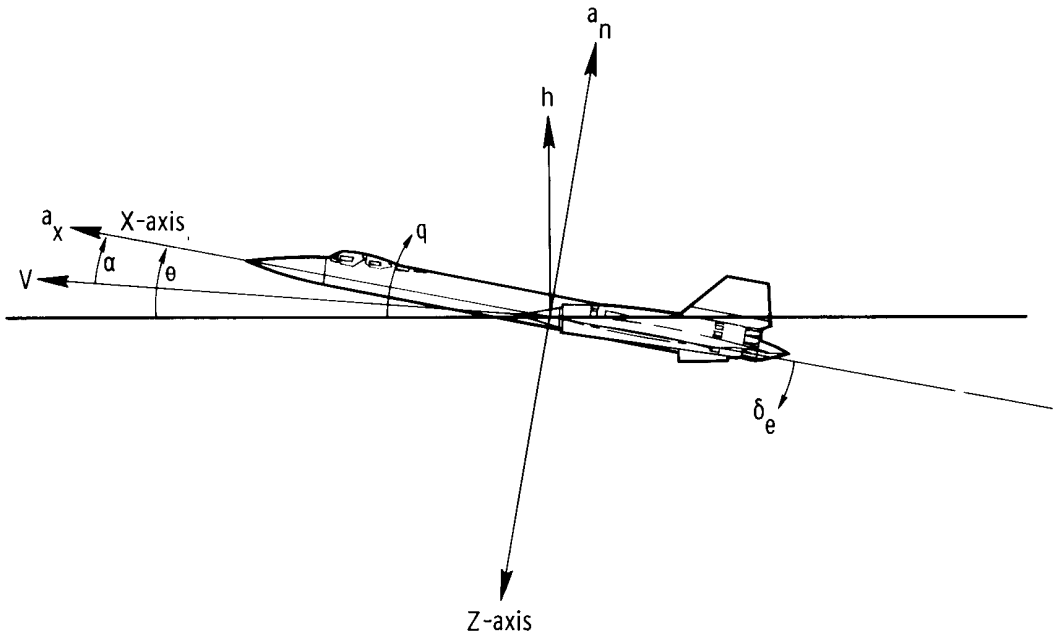

Figure 4. Axis system. Arrows indicate positive directions of values.

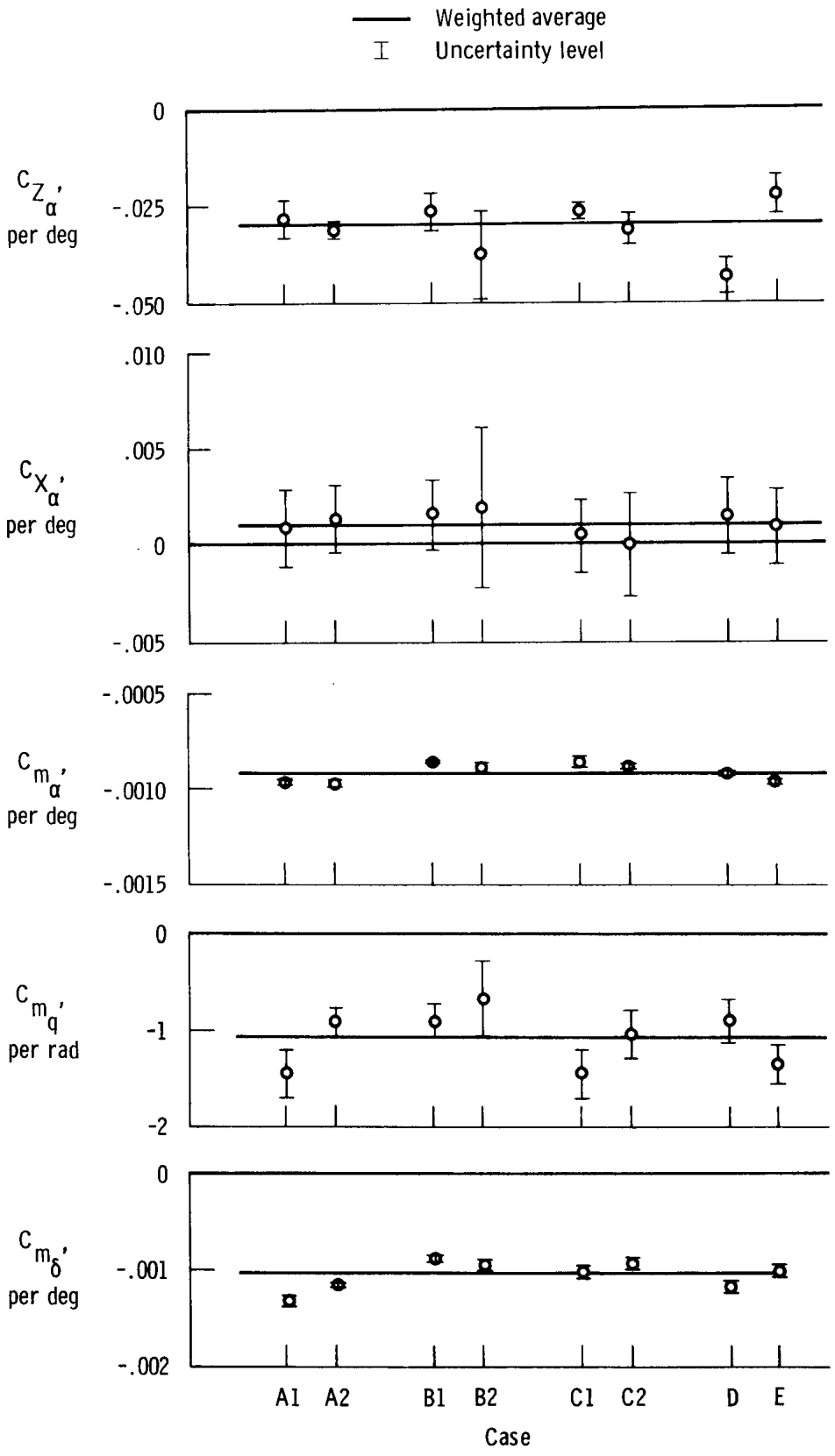

Figure 5. Short-period derivatives. $M \approx 2.9$.

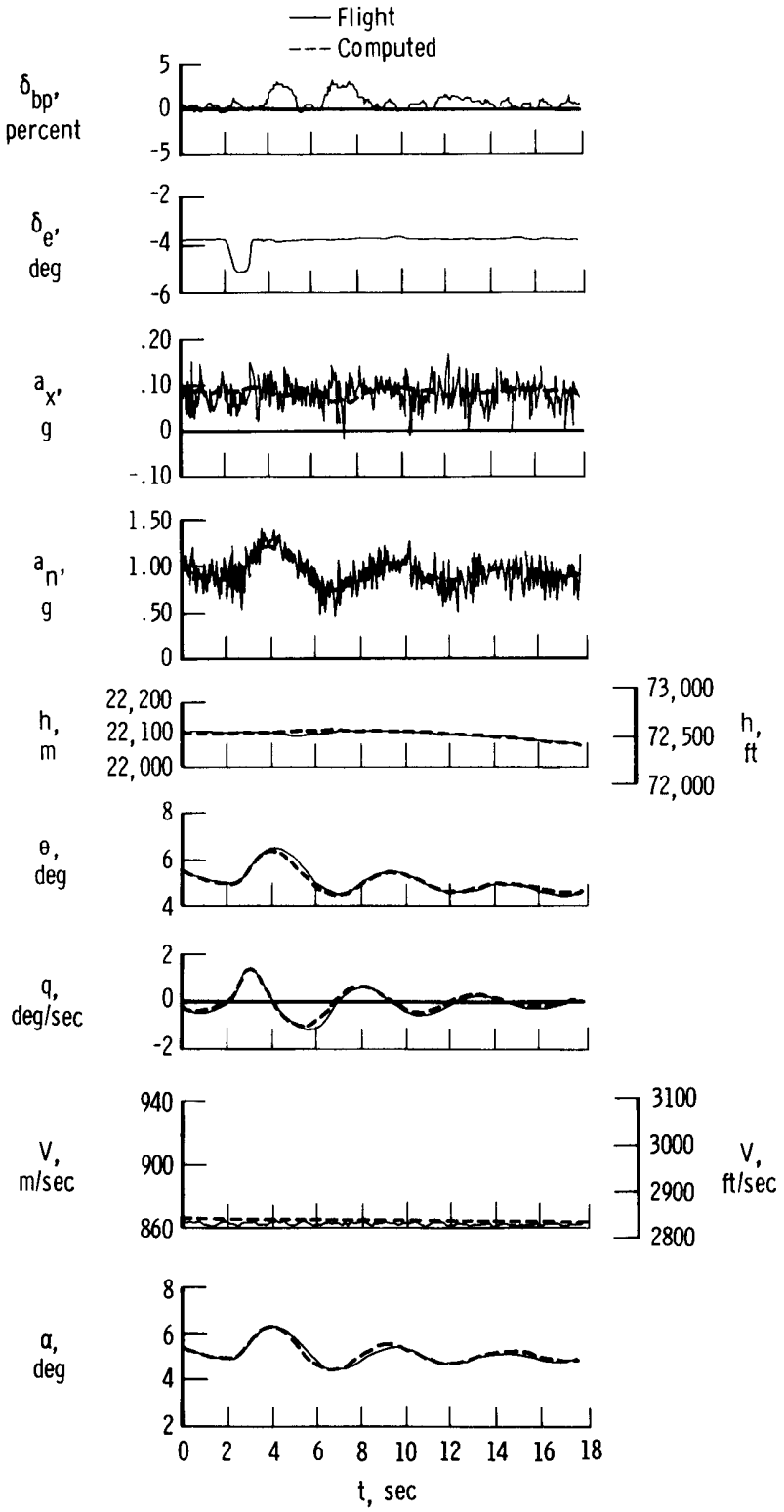

Figure 6. Typical short-period match using average derivatives. Case A1.

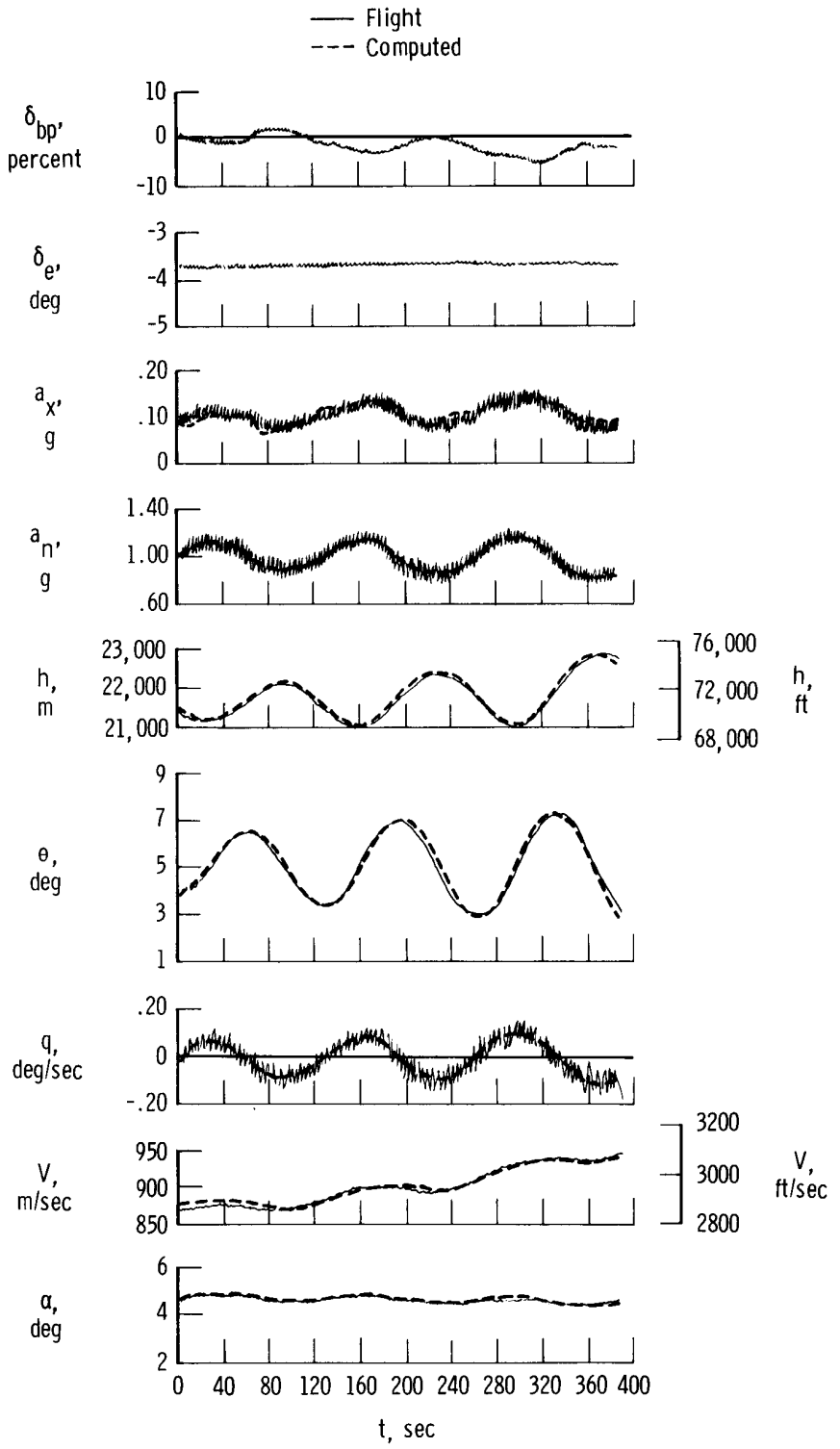

(a) Phugoid case A.

Figure 7. Comparison of flight and computed time histories for phugoid maneuvers.

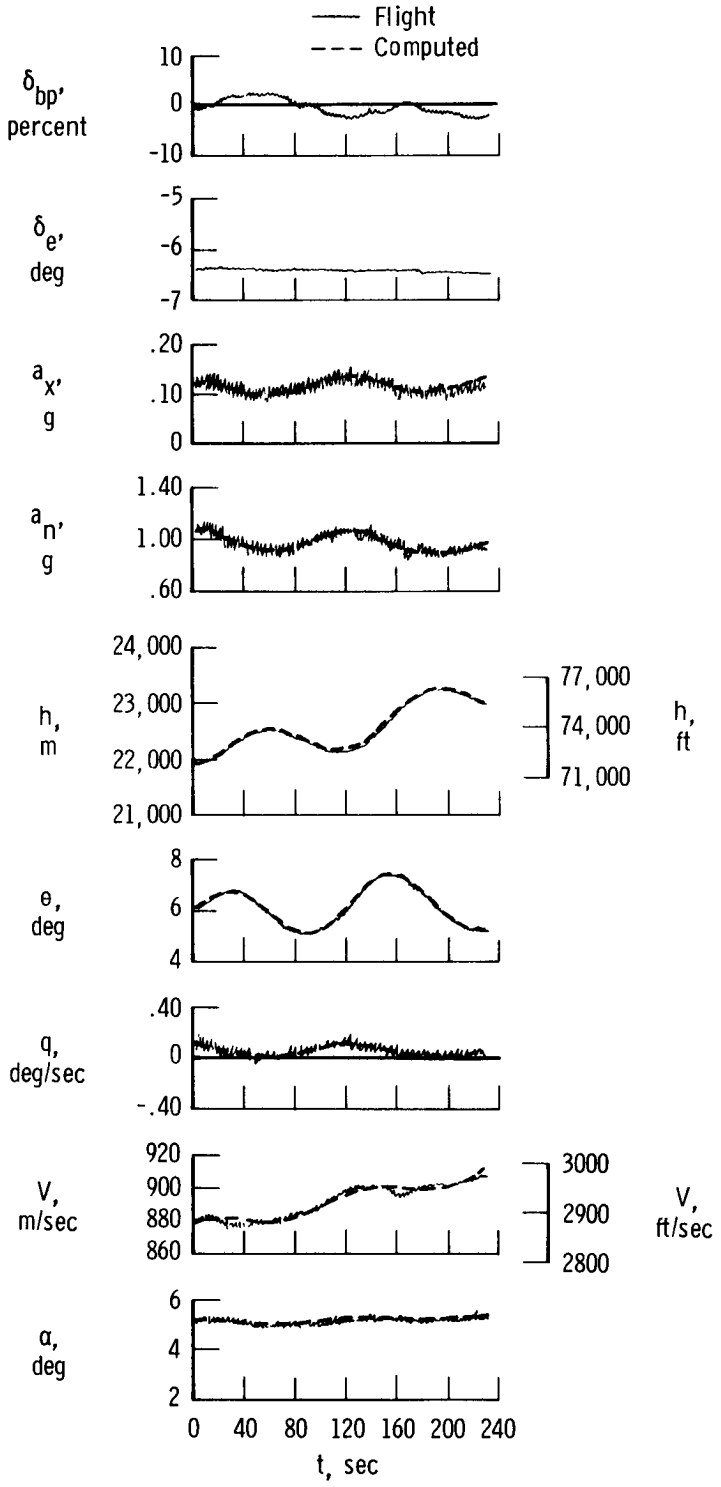

(b) Phugoid case B.

Figure 7. Continued.

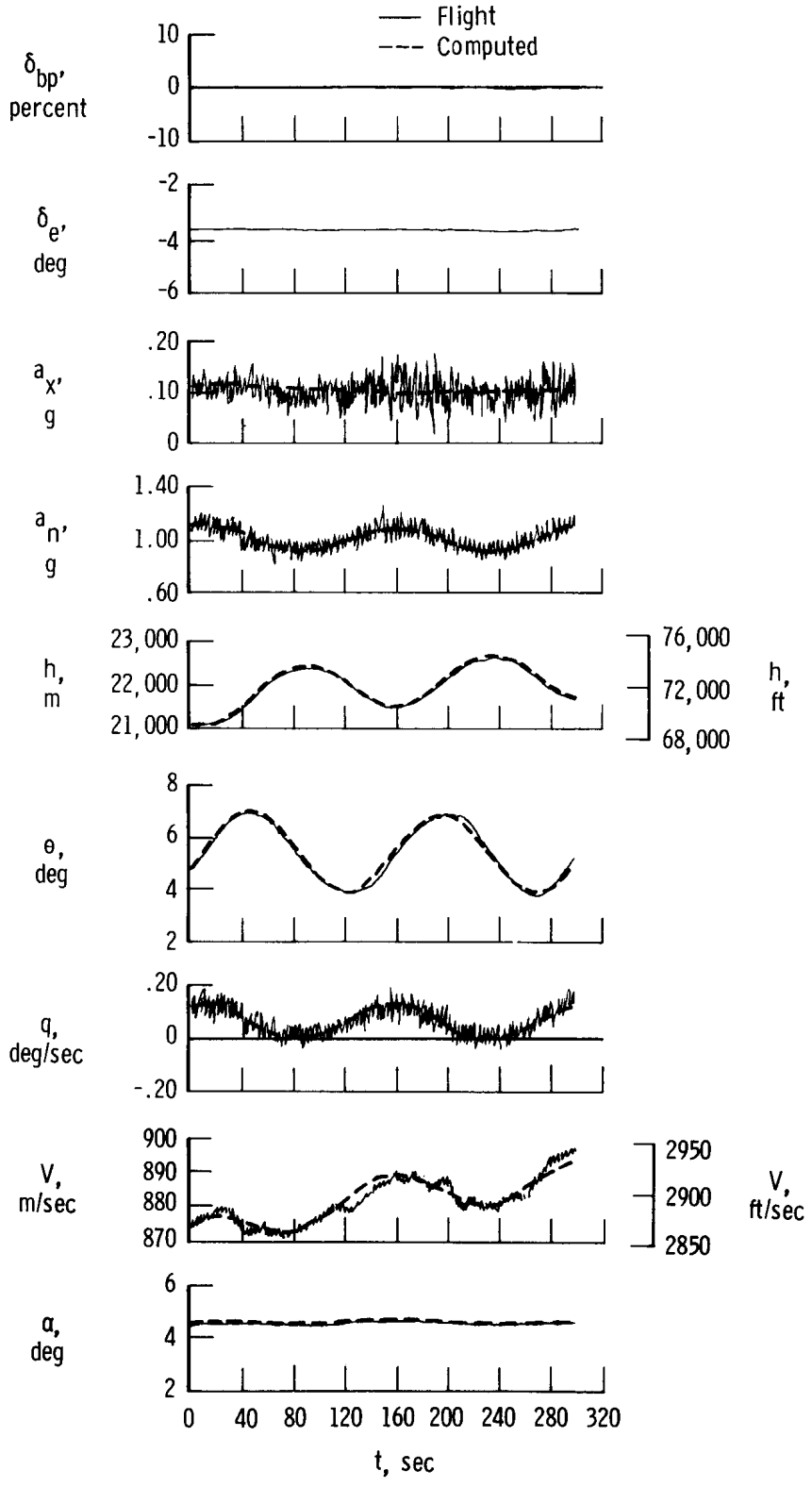

(c) Phugoid case C.

Figure 7. Concluded.

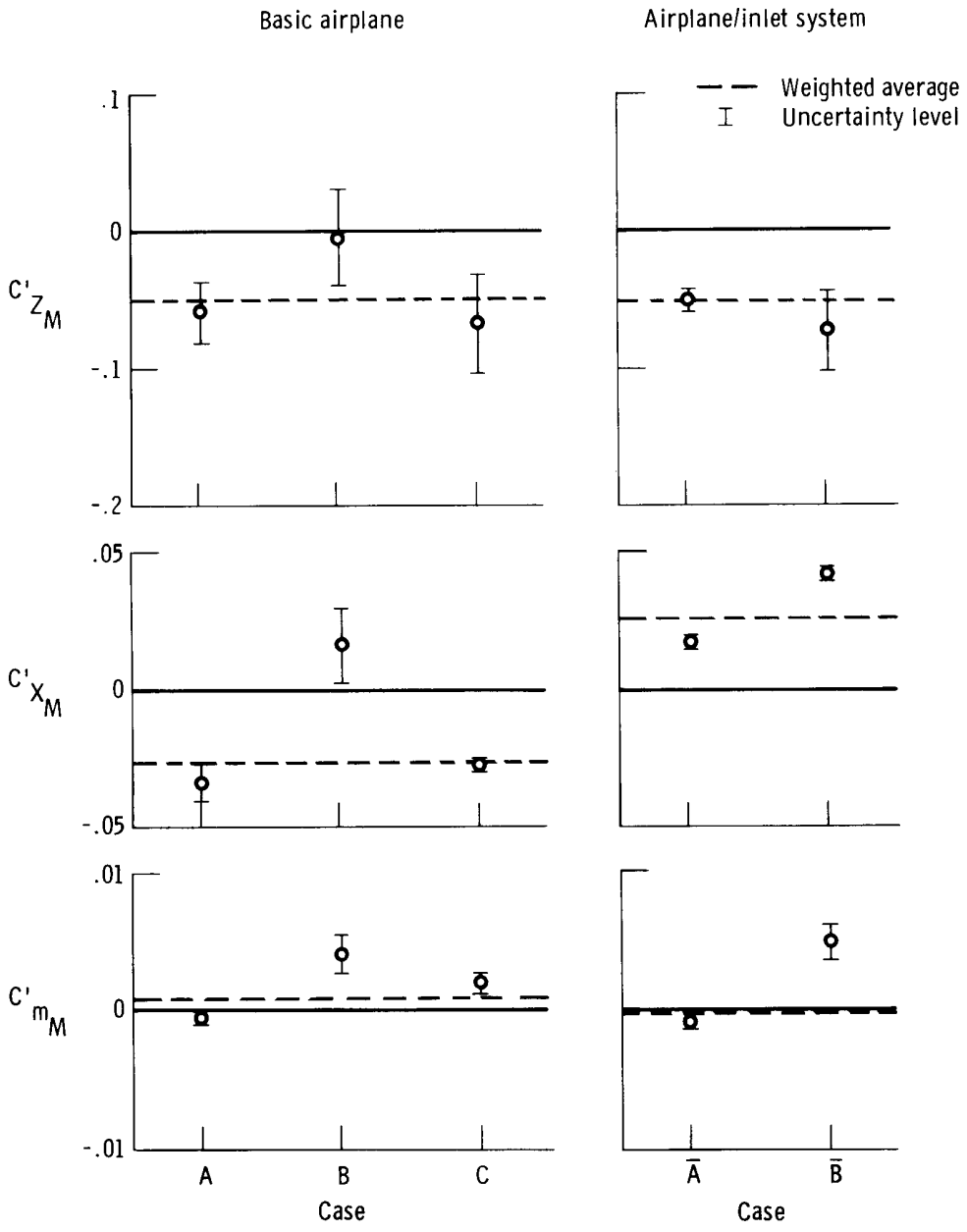

Figure 8. Velocity and altitude derivatives obtained from phugoid maneuvers.

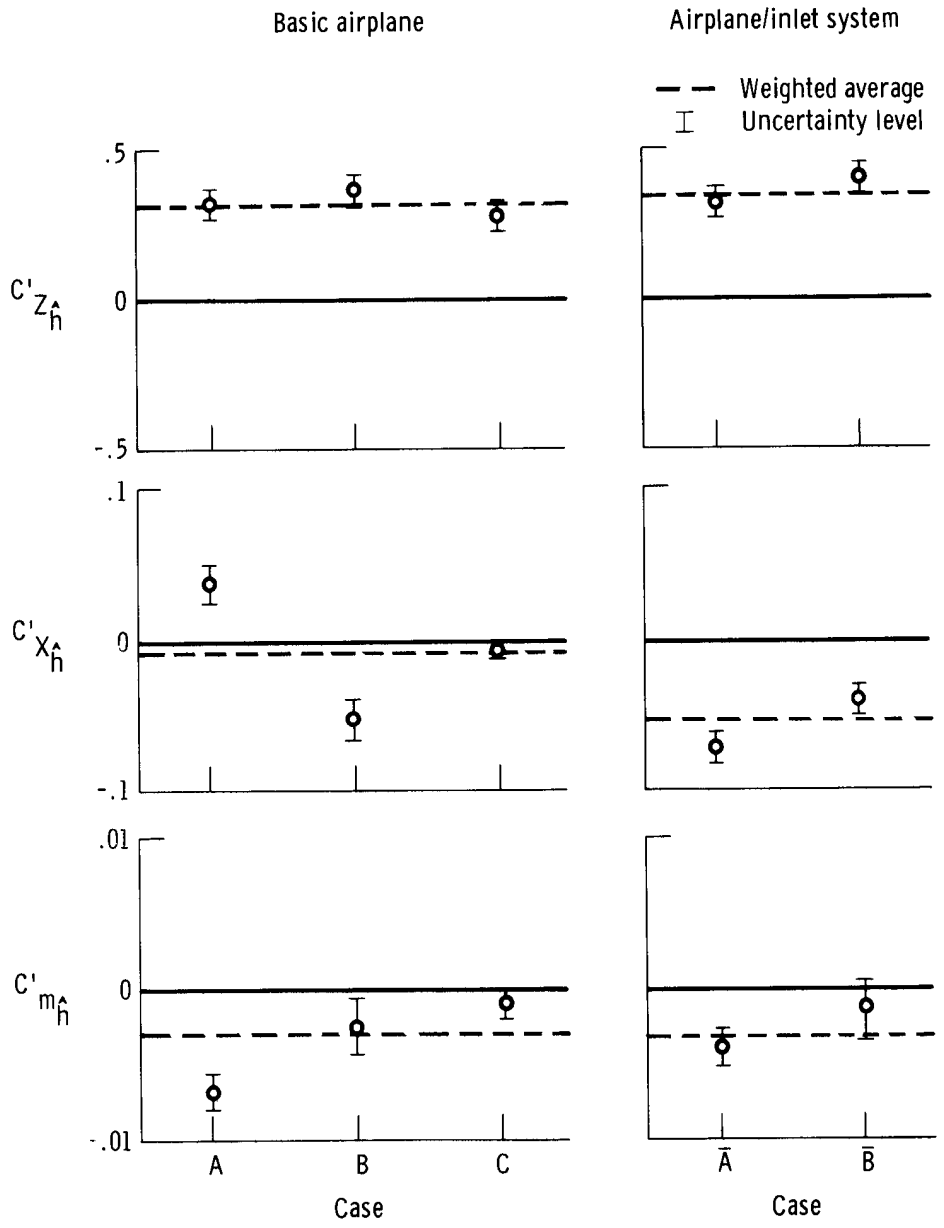

Figure 8. Concluded.

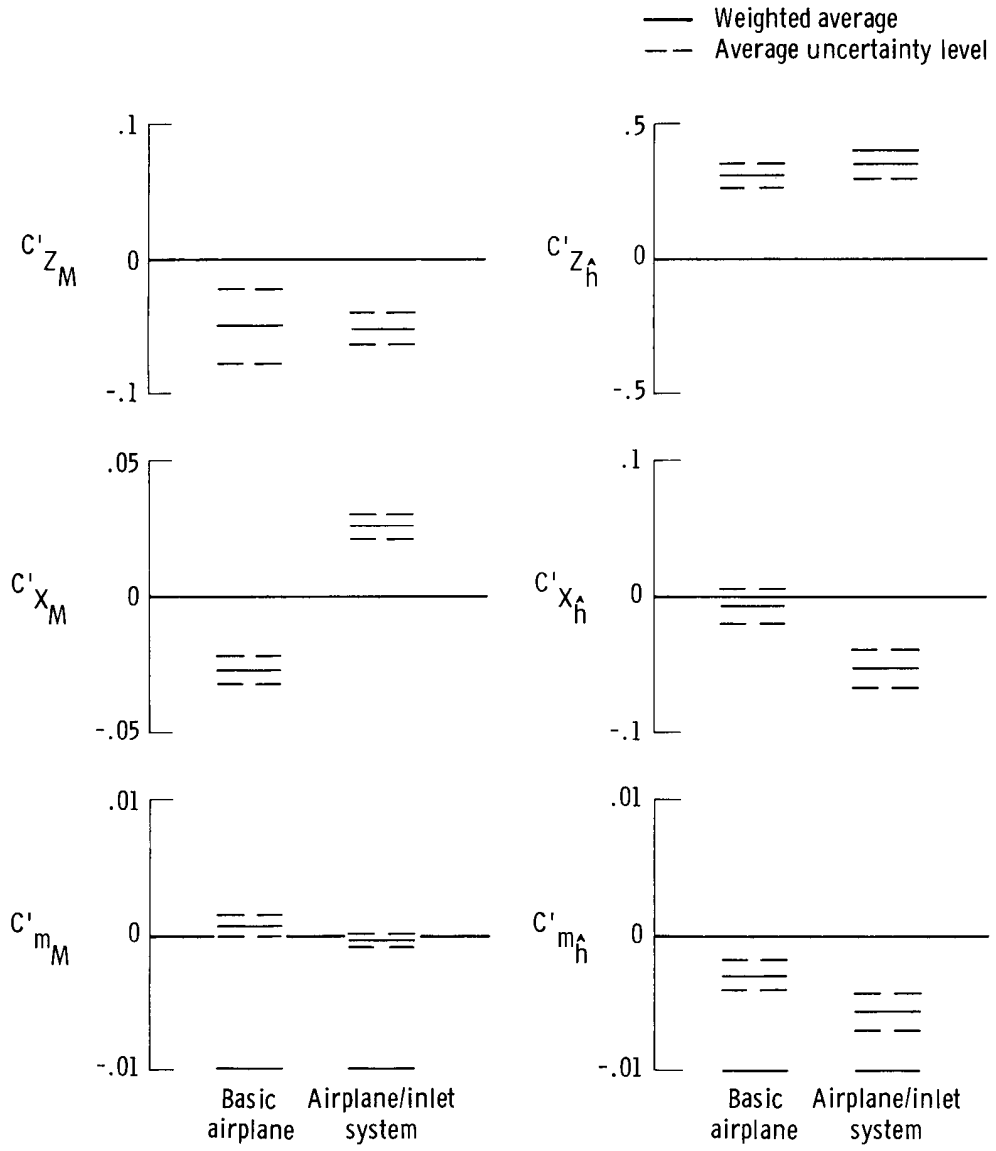

Figure 9. Summary of velocity and altitude derivatives and average uncertainties for $M \approx 2.9$, $h \approx 21{,}900$ m (72,000 ft).

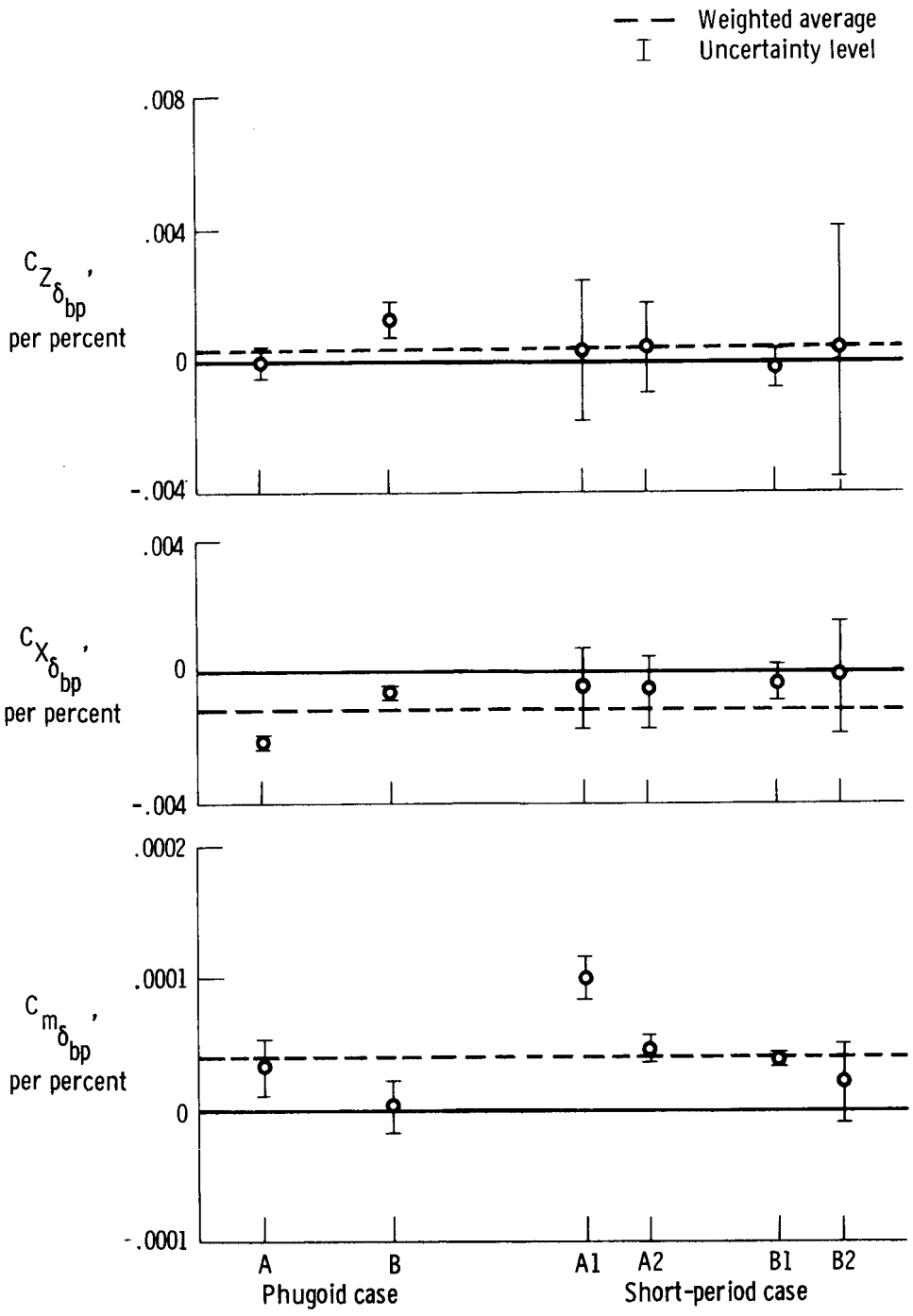

Figure 10. Inlet derivatives.

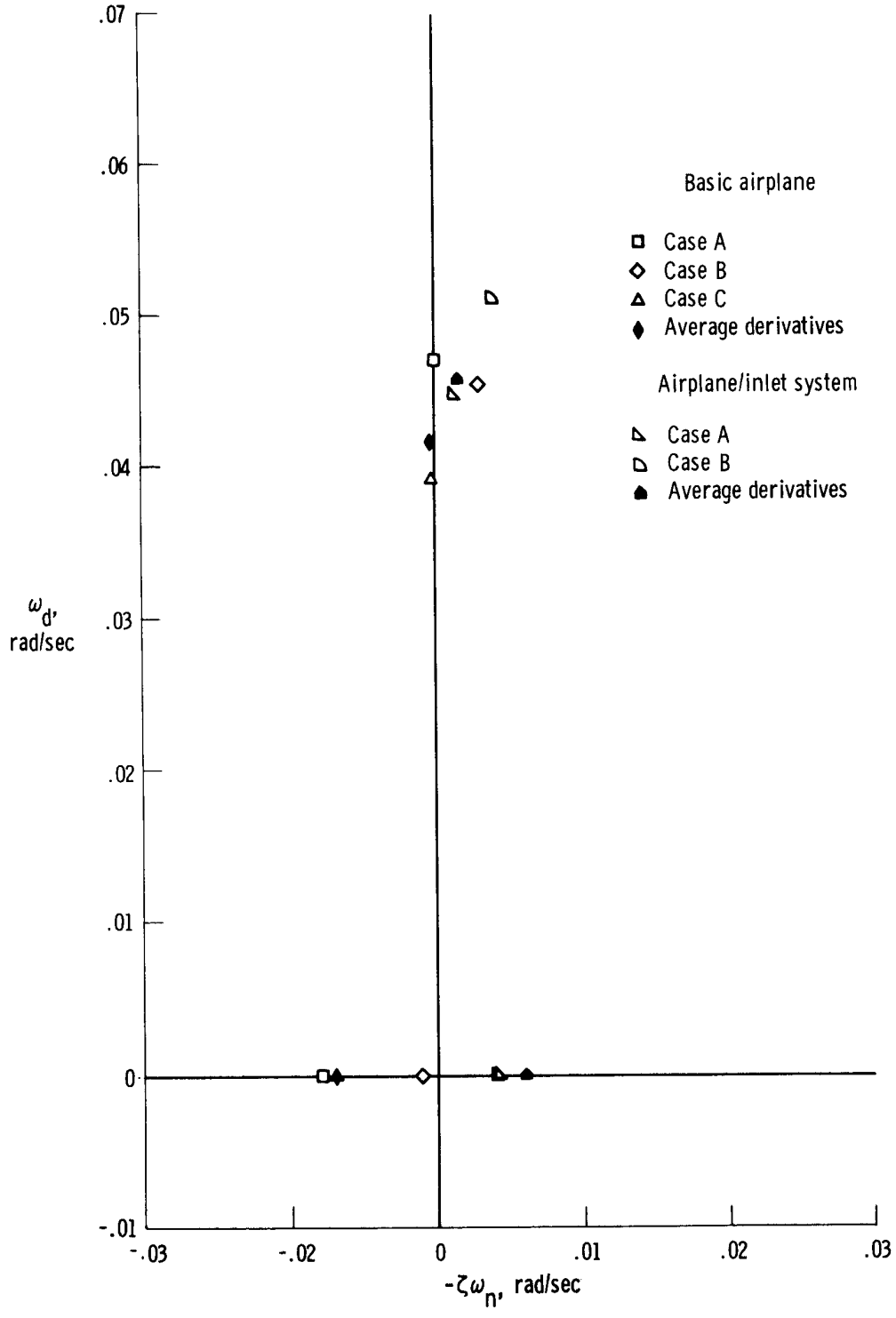

Figure 11. Phugoid and height mode roots for individual cases and weighted average derivatives from figure 8 for M = 2.9 and h = 21,900 m (72,000 ft).

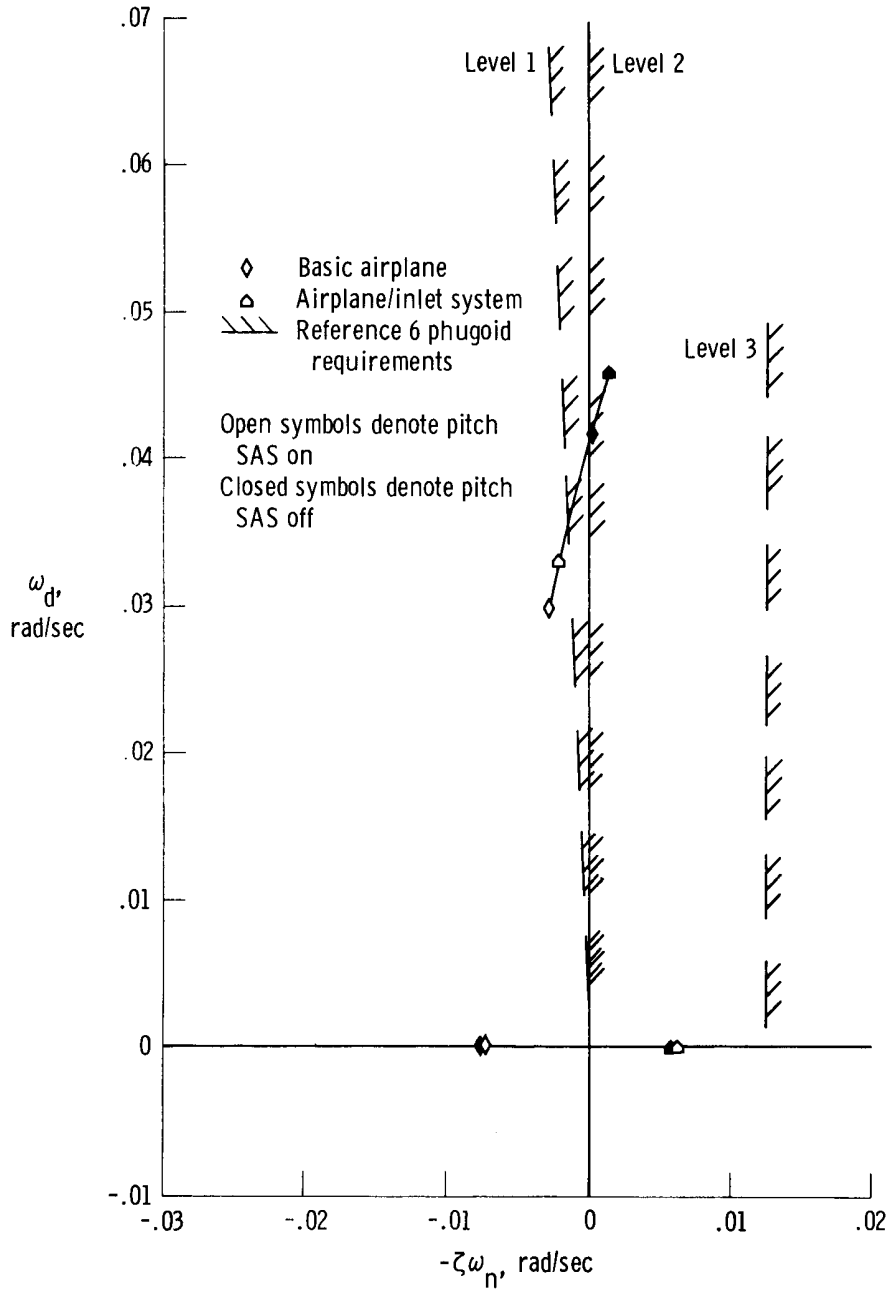

Figure 12. Root locus of pitch stability augmentation system feedback for phugoid and height mode roots. Linear control system.

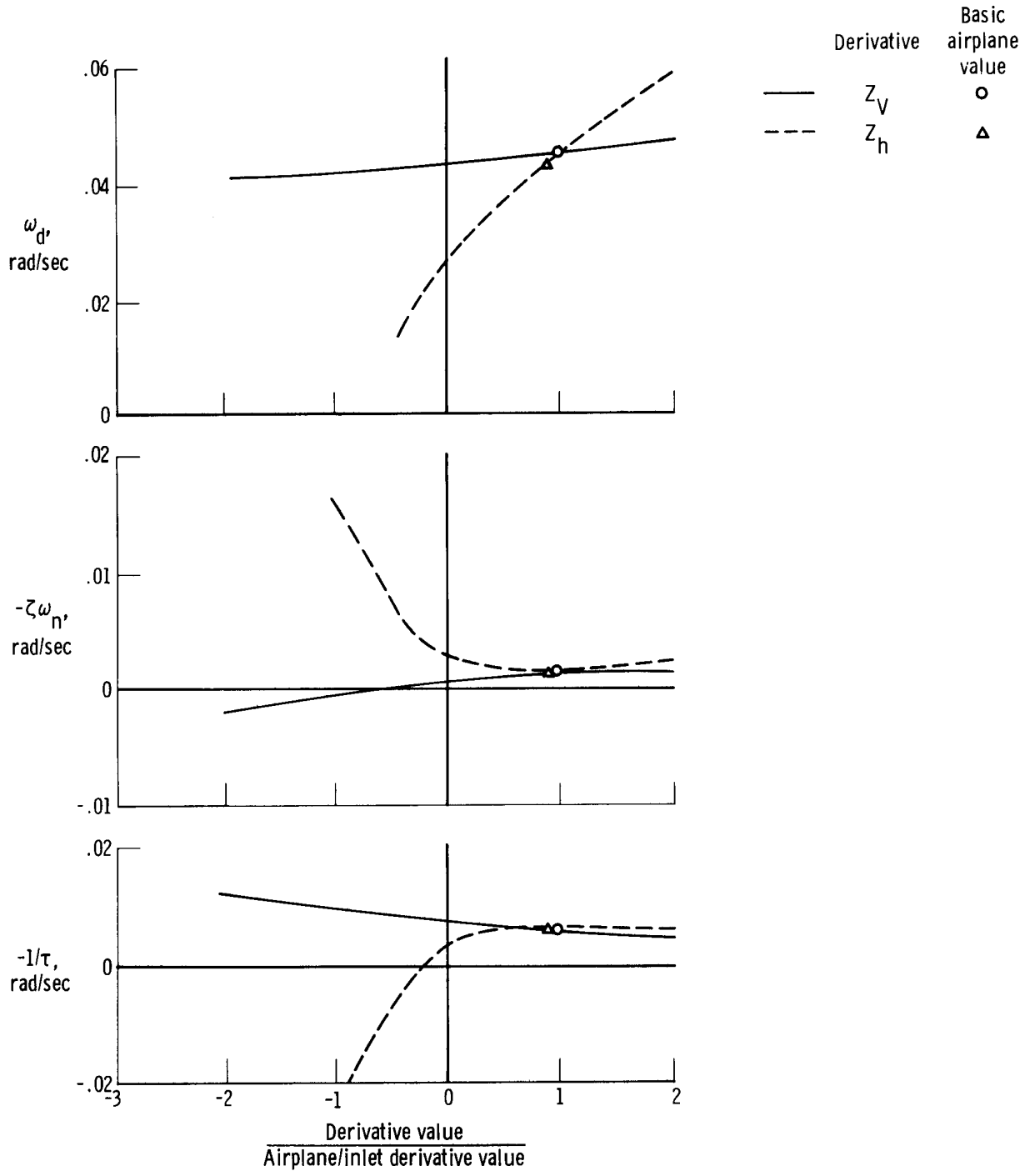

(a) Z_V *and* Z_h.

Figure 13. Phugoid and height mode characteristics as a function of velocity and altitude derivative values.

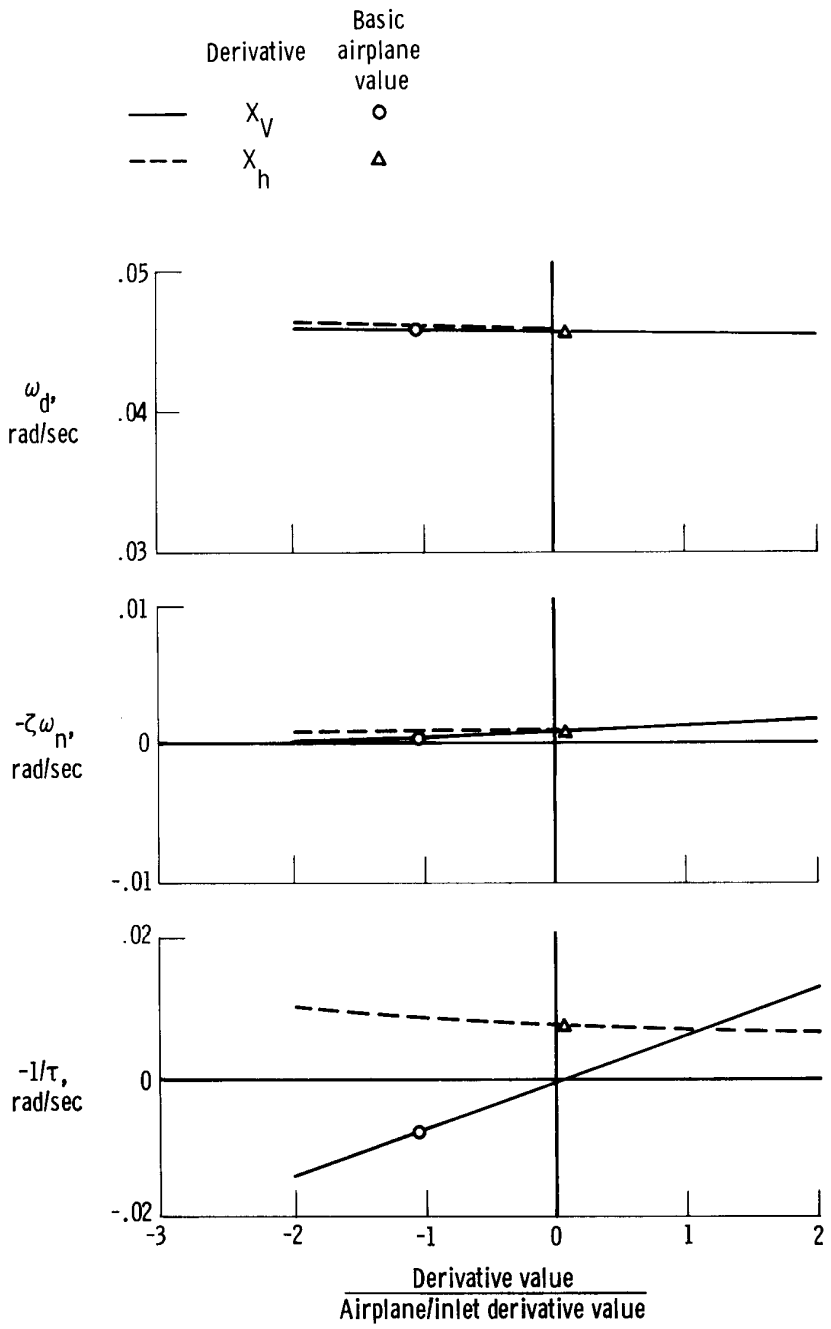

(b) X_V *and* X_h.

Figure 13. Continued.

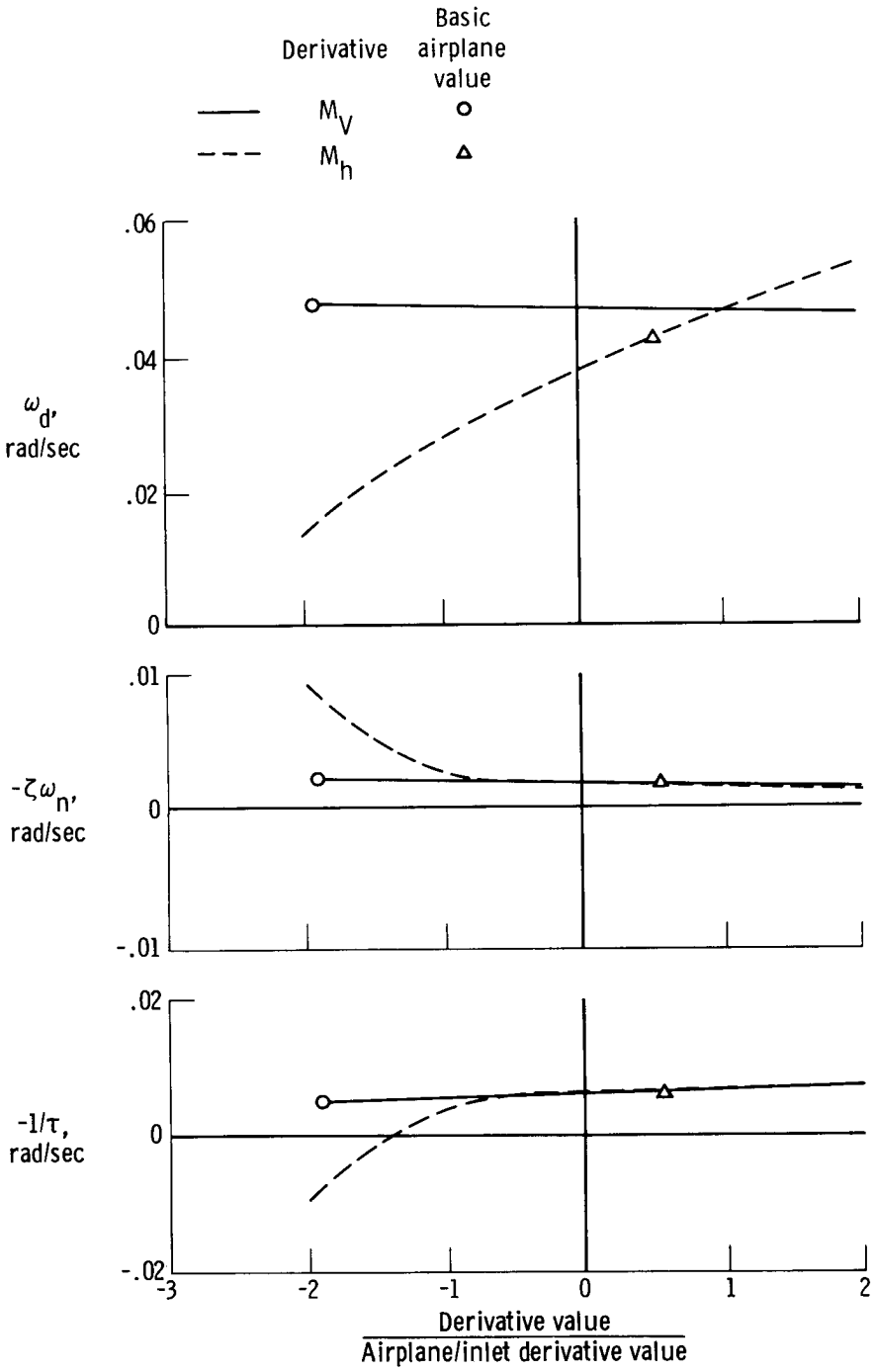

(c) M_V and M_h.

Figure 13. Concluded.

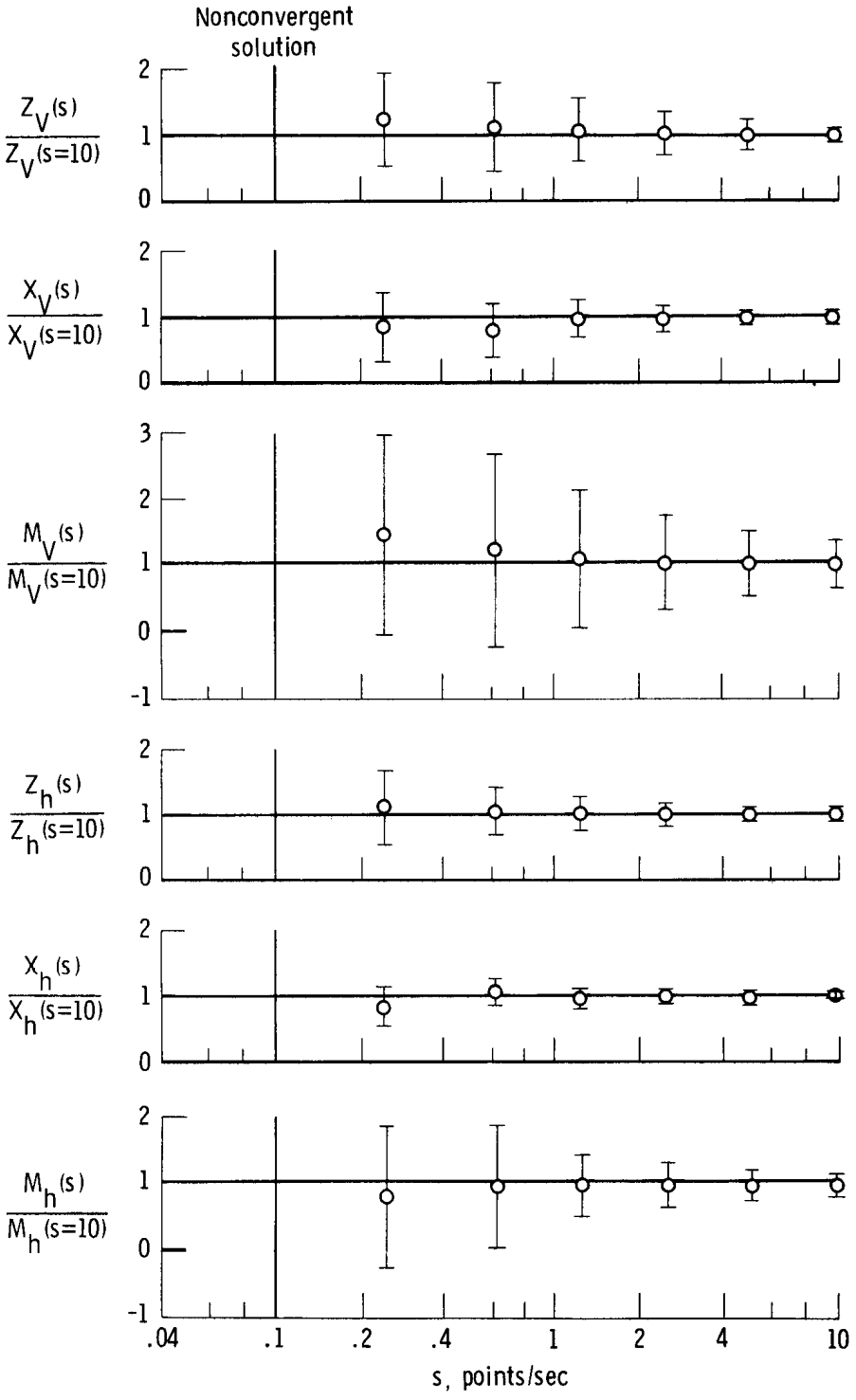

Figure 14. Effect of sampling rate on velocity and altitude derivatives for phugoid maneuver $\bar{A}$.

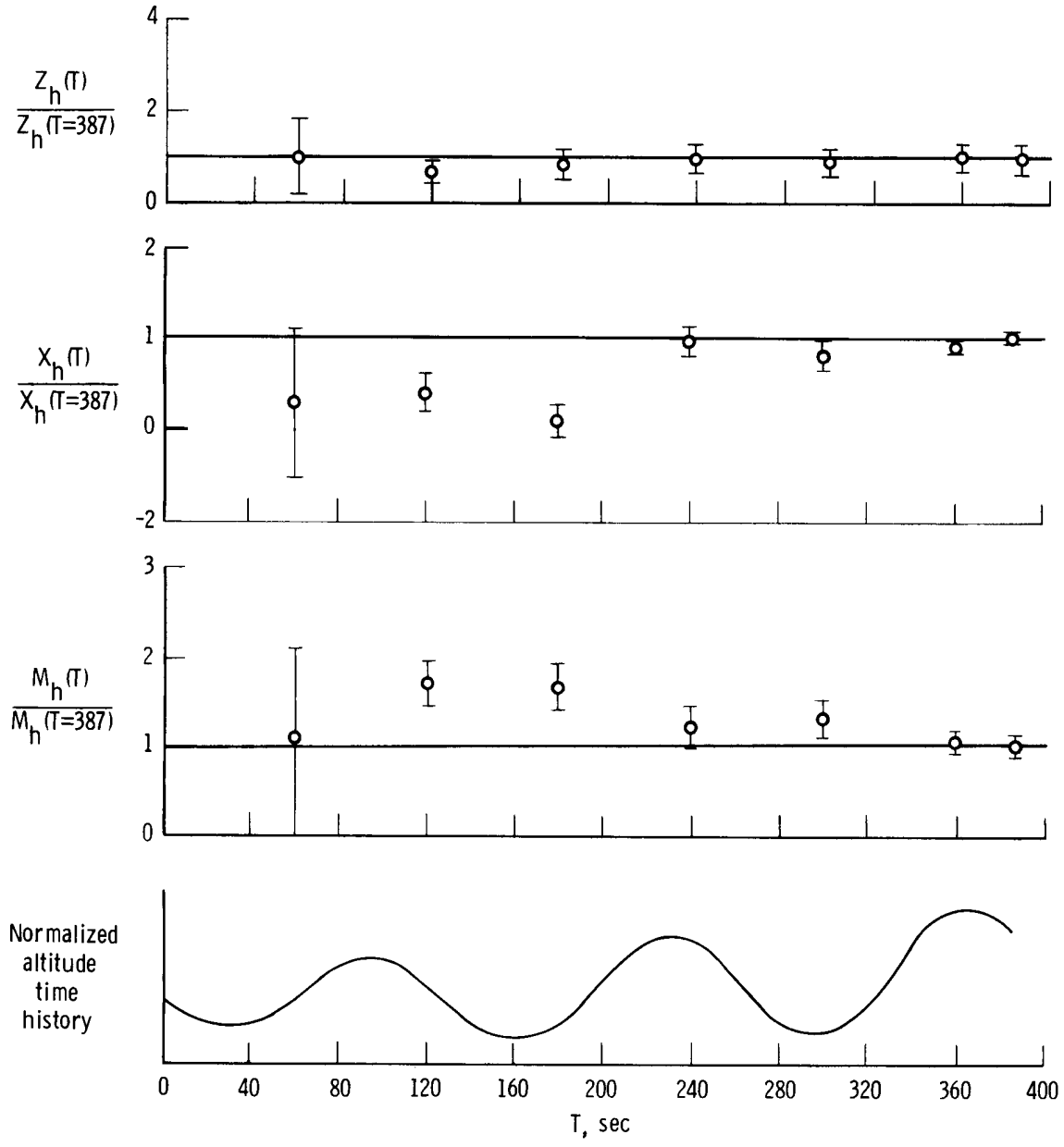

Figure 15. Effect of observation time on velocity and altitude derivatives for fixed sample rate of 2 points per second with phugoid maneuver $\bar{A}$. (Derivatives shown at T correspond to observation of time history from 0 to T.)

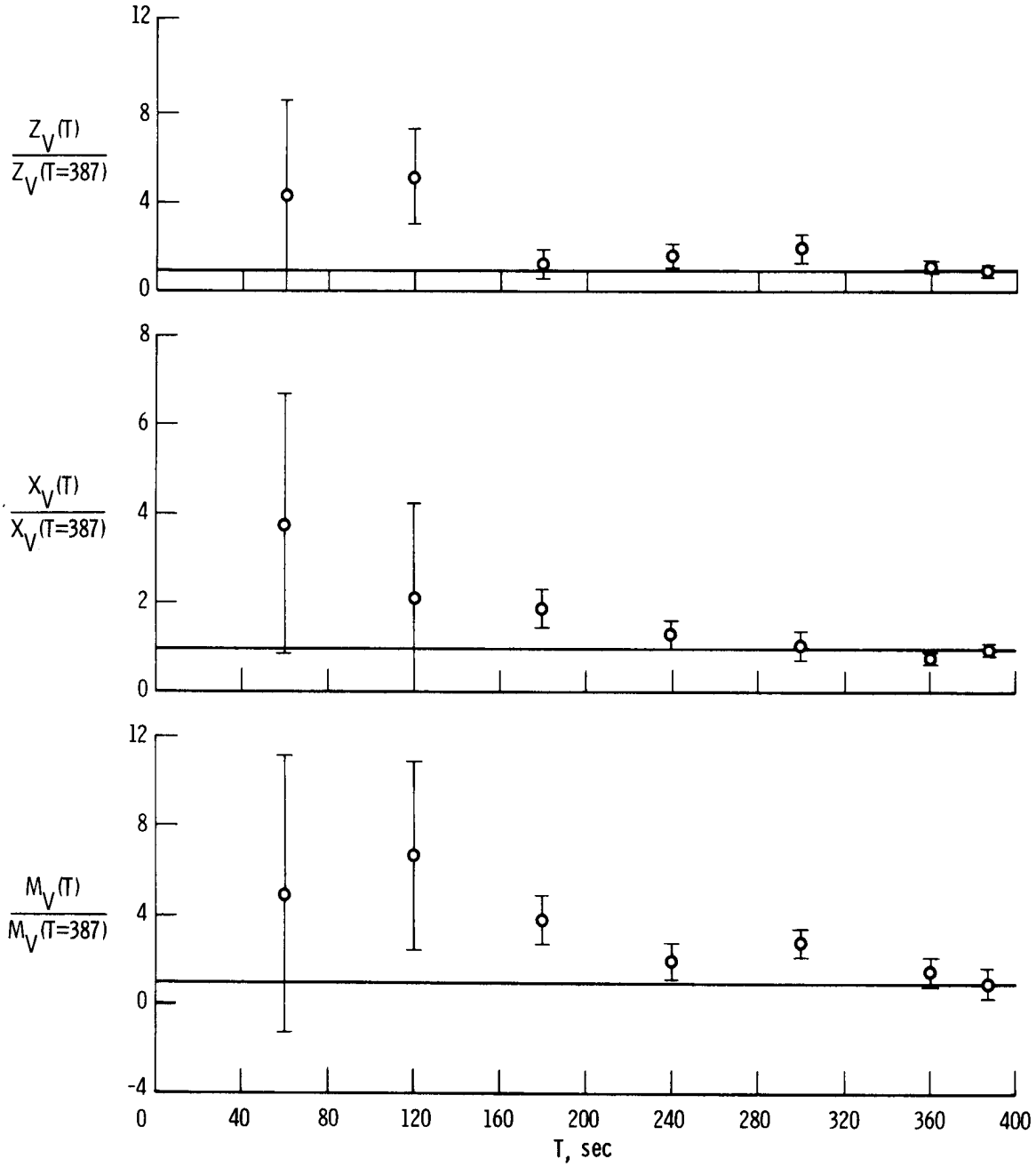

Figure 15. Concluded.

1. Report No.	2. Government Accession No.	3. Recipient's Catalog No.
NASA TP-1107		

4. Title and Subtitle	5. Report Date
PHUGOID CHARACTERISTICS OF A YF-12 AIRPLANE WITH VARIABLE-GEOMETRY INLETS OBTAINED IN FLIGHT TESTS AT A MACH NUMBER OF 2.9	November 1977
	6. Performing Organization Code
7. Author(s)	8. Performing Organization Report No.
Bruce G. Powers	H-953
	10. Work Unit No.
9. Performing Organization Name and Address	505-06-91
Dryden Flight Research Center P. O. Box 273 Edwards, California 93523	11. Contract or Grant No.
	13. Type of Report and Period Covered
12. Sponsoring Agency Name and Address	Technical Paper
National Aeronautics and Space Administration Washington, D.C. 20546	14. Sponsoring Agency Code

15. Supplementary Notes

16. Abstract

Flight tests were conducted with the YF-12 airplane to examine the airplane's longitudinal characteristics at a Mach number of approximately 2.9. Phugoid oscillations as well as short-period pulses were analyzed with the variable-geometry engine inlets in the fixed and the automatic configurations. Stability and control derivatives for the velocity and altitude degrees of freedom and the standard short-period derivatives were obtained. Inlet bypass door position was successfully used to represent the total inlet system, and the effect of the inlets on the velocity and altitude derivatives was determined.

The phugoid mode of the basic airplane (fixed inlet configuration) had neutral damping, and the height mode was stable. With the addition of the inlets in the automatic configuration, the phugoid mode was slightly divergent and the height mode was divergent with a time to double amplitude of about 114 seconds. The results of the derivative estimation indicated that the change in the height mode characteristics was primarily the result of the change in the longitudinal force derivative with respect to velocity. The net propulsive force of the basic airplane decreased with increasing velocity; the net propulsive force of the airplane/inlet system increased with increased velocity.

17. Key Words (Suggested by Author(s))	18. Distribution Statement
Phugoid characteristics Stability and control derivatives Derivatives Height mode YF-12 airplane	Unclassified - Unlimited Category: 08

19. Security Classif. (of this report)	20. Security Classif. (of this page)	21. No. of Pages	22. Price*
Unclassified	Unclassified	44	$3.75

For sale by the National Technical Information Service, Springfield, Virginia 22161

NASA-Langley, 1977